Brain, Behavior, & Immunity - Health 23 (2022) 100473

Contents lists available at ScienceDirect

Brain, Behavior, & Immunity - Health

journal homepage: www.editorialmanager.com/bbih/default.aspx

Interleukin 15 modulates the effects of poly I:C maternal immune activation on offspring behaviour

Faraj L. Haddad [a], Salonee V. Patel [a], Ella E. Doornaert [a], Cleusa De Oliveira [a], Brian L. Allman [a], Kelly J. Baines [a], Stephen J. Renaud [a], Susanne Schmid [a,b,*]

[a] Anatomy & Cell Biology, Schulich School of Medicine & Dentistry, Canada
[b] Department of Psychology, The University of Western Ontario, ON, Canada

ARTICLE INFO

Keywords:
Maternal immune activation
Pregnancy
Poly I:C
Interleukin 15
Startle
Autism spectrum disorder
Schizophrenia
Age
Social behaviour
Anxiety

ABSTRACT

Maternal infections during pregnancy are linked with an increased risk for disorders like Autism Spectrum Disorder and schizophrenia in the offspring. Although precise mechanisms are still unclear, clinical and preclinical evidence suggest a strong role for maternal immune activation (MIA) in the neurodevelopmental disruptions caused by maternal infection. Previously, studies using the Polyinosinic:Polycytidylic (Poly I:C) MIA preclinical model showed that cytokines like Interleukin 6 (Il6) are important mediators of MIA's effects. In this study, we hypothesized that Il15 may similarly act as a mediator of Poly I:C MIA, given its role in the antiviral immune response. To test this hypothesis, we induced Poly I:C MIA at gestational day 9.5 in wildtype (*WT*) and *Il15*$^{-/-}$ rat dams and tested their offspring in adolescence and adulthood. Poly I:C MIA and Il15 knockout produced both independent and synergistic effects on offspring behaviour. Poly I:C MIA decreased startle reactivity in adult *WT* offspring but resulted in increased adolescent anxiety and decreased adult locomotor activity in *Il15*$^{-/-}$ offspring. In addition, Poly I:C MIA led to genotype-independent effects on locomotor activity and prepulse inhibition. Finally, we showed that *Il15*$^{-/-}$ offspring exhibit distinct phenotypes that were unrelated to Poly I:C MIA including altered startle reactivity, locomotion and signal transduction in the auditory brainstem. Overall, our findings indicate that the lack of Il15 can leave offspring either more or less susceptible to Poly I:C MIA, depending on the phenotype in question. Future studies should examine the contribution of fetal versus maternal Il15 in MIA to determine the precise developmental mechanisms underlying these changes.

1. Introduction

Maternal infections during pregnancy are linked with an increased risk for disorders like Autism Spectrum Disorder (ASD) and schizophrenia in the offspring (Jiang et al., 2016; Khandaker et al., 2013). Factors that modulate the association between maternal infection and offspring risk of neurodevelopmental disorders have been previously summarized by our group and others. These include the timing of infection, severity of infection, and presence of other risk factors (Haddad et al., 2020b; Han et al., 2021). Offspring risk for neurodevelopmental disorders increases greatly if infection occurs in the first half of pregnancy (Atladóttir et al., 2010; Brown et al., 2000, 2004a; Sørensen et al., 2009) and if the infection is severe, leading to more hospital visits and higher concentrations of circulating inflammatory factors (Atladóttir et al., 2012; Brown et al., 2014; Fang et al., 2015; Hornig et al., 2018; Koks et al., 2016; Mortensen et al., 2007). Furthermore, it also increases if there is family history of psychiatric disorders, or if offspring go on to experience peripubertal trauma (Blomström et al., 2016; Clarke et al., 2009; Debost et al., 2017).

Since several bacterial and viral maternal infections show these associations with neurodevelopmental disorders, it is thought that the maternal immune response disrupts neurodevelopment independently from pathogen-specific effects. Indeed, increased maternal cytokine levels during pregnancy have been correlated with the degree of offspring risk for developing ASD and schizophrenia (Abdallah et al., 2013; Allswede et al., 2016; Brown et al., 2004b; Ellman et al., 2010; Goldstein et al., 2014; Jones et al., 2017; Zerbo et al., 2014).

In addition, preclinical models suggest that maternal immune activation (MIA) during pregnancy in the absence of a pathogen leads to neurodevelopmental disruption, which is associated with ASD and schizophrenia-related brain and behavioural changes in the offspring (Haddad et al., 2020b; Solek et al., 2018). In rodents, MIA is typically

* Corresponding author. Anatomy & Cell Biology, Schulich School of Medicine & Dentistry, 1151 Richmond Street, London, ON, N6A 3K7, Canada.
E-mail address: Susanne.schmid@schulich.uwo.ca (S. Schmid).

https://doi.org/10.1016/j.bbih.2022.100473
Received 13 May 2022; Accepted 14 May 2022
Available online 18 May 2022

induced by injection of Polyinosinic:Polycytidylic acid (Poly I:C), an analog of viral double-stranded RNA, which elicits an innate immune response by binding to the innate immune receptor Toll-like receptor 3 (Fitzgerald et al., 2003).

Although preclinical MIA models have shown considerable face and predictive validity, the mechanisms underlying the effects of MIA on the fetal brain are still unclear. Previous reports implicate cytokines such as Interleukin 6 (Il6), Il10, and Il17 as important mediators of the effects of MIA on offspring behavioural phenotypes (Il6: Lipina et al., 2013; Pineda et al., 2013; Pratt et al., 2013; Smith et al., 2007; Il10: Meyer et al., 2008; Il17: Kim et al., 2017; Lammert et al., 2018; Schwartzer et al., 2013; Shin Yim et al., 2017). However, the immune response following MIA leads to changes in the peripheral levels of many other cytokines and chemokines (Arrode-Brusés and Brusés, 2012; Careaga et al., 2018).

Il15 is a cytokine that could be implicated in the effects of Poly I:C MIA on the fetal brain due to its role in immunity and placental development. However, it has not yet been studied in the context of MIA-linked neurodevelopmental disorders. One of the primary roles of Il15 involves immune regulation within the antiviral immune response. Il15 is found in high concentrations mainly in immune cells such as dendritic cells, monocytes, and macrophages (Perera et al., 2012). In macrophages, Il15 regulates the production of proinflammatory cytokines such as Tumor Necrosis Factor (TNF), Il1, and Il6 (Alleva et al., 1997). Beyond its immune regulatory roles, Il15 is required for the development of Natural Killer (NK) cells, as shown by the lack of NK cells in Il15 or Il15Rα-deficient mice (Kennedy et al., 2000; Lodolce et al., 1998). NK cells are cytotoxic innate immune cells found in the circulation and various organs throughout the body (Mandal and Viswanathan, 2015; Shi et al., 2011). Of relevance to pregnancy, NK cells account for a large proportion of uterine leukocytes in early pregnancy and play a role in vascular remodeling during placental development (Renaud et al., 2017; Shi et al., 2011). Elevations in Il15 have been shown after maternal injection of Poly I:C (Arrode-Brusés and Brusés, 2012; Mattei et al., 2001) and changes in circulating Il15 have been detected in Poly I:C offspring blood up to two weeks postnatally (Paraschivescu et al., 2020).

Based on the important role of Il15 in immune regulation and the role of NK cells in the placenta, we hypothesized that the effect of Poly I:C MIA would be diminished in Il15-deficient animals. To test this hypothesis, we induced Poly I:C MIA at GD9.5 in wildtype (*WT*) and in Il15 knockout (*Il15*$^{-/-}$) dams. The prenatal timepoint, dose of Poly I:C, and method of administration are commonly used in a large proportion of Poly I:C studies (Haddad et al., 2020b), including a previous study conducted by our group (Haddad et al., 2020a), which reported increased adult startle reactivity in GD9.5 but not GD14.5 Poly I:C offspring. In addition to startle phenotypes that provide measures of sensory processing and sensory filtering, we also tested locomotor activity and social behaviour. The behavioural domains covered by our battery of tests are typically affected in humans with autism and schizophrenia and in animal models with neurodevelopmental disorders in general, especially Poly I:C models (Haddad et al., 2020b).

2. Materials and methods

2.1. Animals

This study was conducted using *WT* or *Il15*$^{-/-}$ male and female Holtzman Sprague-Dawley rats. The generation of these rats was described previously by Renaud et al. (2017). In brief, using zinc finger nuclease-mediated genome editing, a 7 base pair frameshift deletion was created within the second exon of *Il15*. The frameshift created a premature stop codon resulting in a truncated protein, and rats homozygous for this mutation showed greatly reduced numbers of NK cells, the survival of which requires functional Il15 signaling (Renaud et al., 2017). Rats were housed in open cages with corn cob bedding, given ad libitum food and water, and kept on a 12 hr light – 12 hr dark cycle with lights turning on at 7:00 a.m. Cages were enriched with polycarbonate huts and wrinkled paper and changed weekly. All behavioral testing and cage changes took place during the light phase (between 7:00 and 19:00 hr). Animals were cared for according to the ethical guidelines of the Animal Care Committee at Western University and the Canadian Council on Animal Care.

2.2. Timed breeding

Adult homozygous *WT* or *Il15*$^{-/-}$ male rats were paired with a maximum of two adult females of the same genotype at a time (homozygous breeding). After pairing, a vaginal smear was collected from each female at 8:00 a.m. every morning and inspected under a light microscope to track the estrus cycle and check for the presence of sperm. If sperm was detected in the smear, the female was considered pregnant, and that day was considered as Gestation Day (GD) 0.5. Pregnant females were separated from the male on GD0.5 and transferred into a single cage, where they were left undisturbed until injection day (GD9.5). Each female was only bred once for this study.

2.3. Maternal immune activation

Pregnant *WT* or *Il15*$^{-/-}$ females were randomly assigned to receive either Poly I:C or saline injections. MIA was induced using Poly I:C (Sigma Cat #P0913, Lot#037M4011V), which had been previously aliquoted and stored at −20 °C. The effectiveness of the same batch of Poly I:C was verified in a previous study by measuring proinflammatory cytokine expression in the fetal tissue 6 h after Poly I:C injection, using quantitative reverse transcriptase polymerase chain reaction (Haddad et al., 2020a). Poly I:C aliquots were diluted in 0.9% saline to obtain a concentration of 4 mg/mL. At around 10:00 a.m. on GD9.5, pregnant females were weighed and had their rectal temperature taken. They were injected with either 0.9% saline or 4 mg/kg of Poly I:C into the tail vein under isoflurane anesthesia (5% induction, 2% maintenance). The injection procedure took an average of 10 min after which rats were returned to their cages and left undisturbed besides temperature/weight measurement and weekly cage change. Temperature measurements were taken 6- and 24-hr following injection, whereas maternal weight was recorded 6-, 24- and 48-hr following injection.

The day of parturition was designated as postnatal day (PND) 0. Offspring were weaned at PND21, and littermates were separated based on sex and housed in groups of 2–4 rats per cage. At the end of the experiment, the final number of litters per group was as follows: *WT* saline - 3 litters; *WT* Poly I:C - 4 litters; *Il15*$^{-/-}$ saline - 3 litters; *Il15*$^{-/-}$ Poly I:C - 5 litters. All litters were culled to 3–5 animals per sex per litter at 1 week of age through random selection. The final number of offspring included for analysis per group, sex, and experiment is shown in Table 1.

2.4. Offspring testing outline

Auditory brainstem response (ABR) and behavioural testing occurred in adolescence and adulthood. Adolescent testing started at PND38-39, and adult testing started PND90-100. PND38-39 in laboratory rats marks a time period just after onset of pubertal milestones (Clark and Price, 1981; Korenbrot et al., 1977; Piekarski et al., 2017), and although adolescence is thought to start earlier, it was not suitable to start our long testing battery at earlier timepoints as some tests would fall before and others would fall after pubertal milestones. In addition, our group has previously investigated auditory processing including ABR, startle reactivity, and PPI in a genetic model for ASD and found changes in all 3 phenotypes at PND38-42 (Scott et al., 2018). Since some adolescent brain changes continue to occur into PND60 (Juraska and Willing, 2017), PND90-100 represents a suitable adult testing timepoint when these adolescent changes are more or less complete.

Animals underwent the same tests at each timepoint, with the whole

Table 1
Animal numbers.
The table shows numbers of offspring per group and sex used for each experiment. WT and Il15$^{-/-}$ dams injected with saline or Poly I:C are numbered in the "Litter" column.

	Litter	Adolescent (♂,♀)			Adult (♂,♀)			
		Sociability	Social Novelty	Open Field, Startle	Sociability	Social Novelty	Open Field, Startle	Immuno-staining
WT Saline	1	3,2	3,2	4,2	3,2	3,2	4,2	1,1
	2	3,4	2,4	3,4	2,4	2,4	3,4	2,1
	3	0,3	0,3	0,3	0,3	0,3	0,3	0,2
	Total	6,9	5,9	7,9	5,9	5,9	7,9	3,4
WT Poly I:C	1	3,4	3,4	4,4	3,4	2,4	4,4	1,1
	2	3,2	3,2	2,2	2,2	2,2	2,2	1,1
	3	4,3	4,4	4,3	2,3	3,3	4,3	2,1
	4	3,4	4,3	4,4	3,4	0,4	4,4	1,2
	Total	13,13	14,13	14,13	10,13	7,13	14,13	5,5
Il15$^{-/-}$ Saline	1	4,4	4,4	4,4	2,4	3,4	4,4	1,1
	2	1,3	2,3	4,3	1,3	3,3	4,3	1,1
	3	3,4	3,4	3,4	0,4	1,4	2,4	2,2
	Total	8,11	9,11	11,11	3,11	7,11	10,11	4,4
Il15$^{-/-}$Poly I:C	1	4,4	4,4	4,4	2,4	3,4	4,4	1,1
	2	3,4	4,4	4,4	3,4	3,4	4,4	1,2
	3	3,4	3,4	4,4	2,4	3,4	4,4	1,1
	4	4,4	4,4	4,4	4,4	2,4	4,4	1,1
	5	2,4	2,4	2,4	1,4	2,4	2,4	1,1
	Total	16,20	17,20	18,20	12,20	13,20	18,20	5,6

battery of ABR and behavioural tests taking about 10 days to complete. Tests were performed in the following order: Startle acclimation and handling (Day 1), ABR measurements (Days 2 & 3), social behaviour testing (Days 4 & 5), open field and startle reactivity testing (Day 6), startle habituation testing (Days 7–10), and PPI testing (Day 11). Due to technical constraints, ABR testing was performed on a subset of animals that underwent behavioural testing (typically two animals per sex per litter). In order to minimize the influence of anesthesia used during ABR

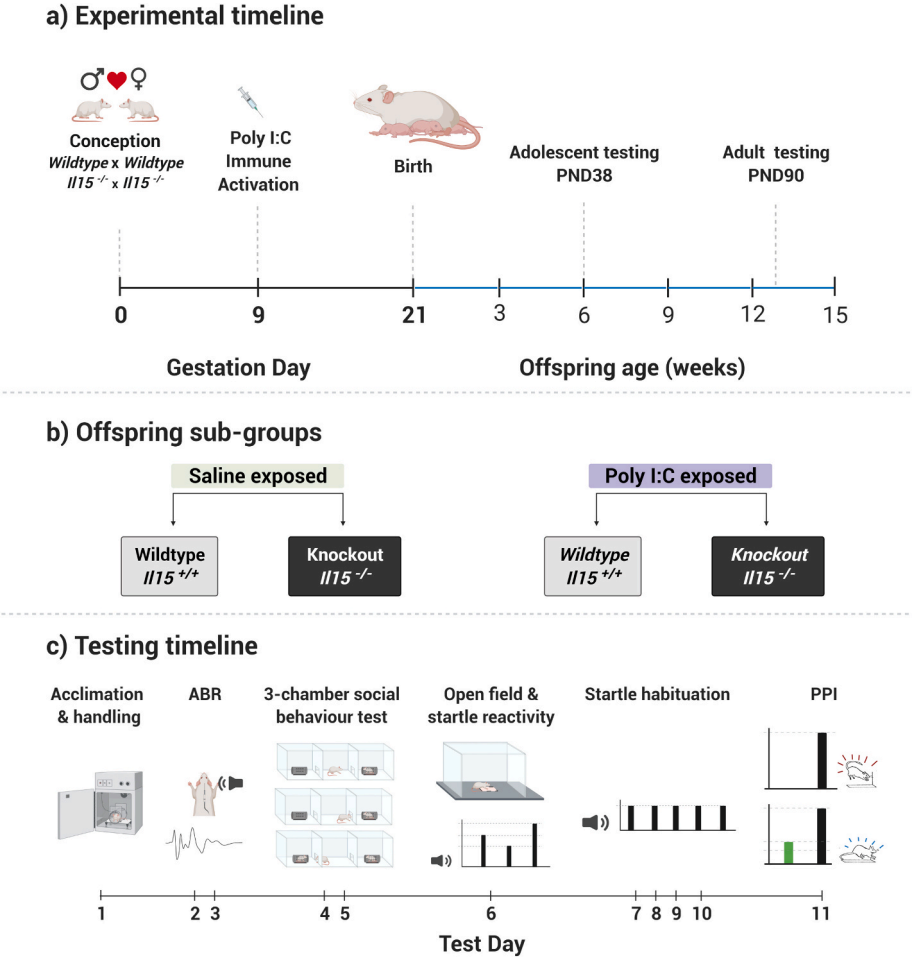

Fig. 1. Overview of the present study including experimental timeline (A), offspring subgroups (B), and within-group testing timeline (C).

testing on behavioural phenotyping, all animals that underwent ABR testing were given one full day to recover prior to social behaviour testing (e.g. if an animal underwent ABR testing on day 2, its social behaviour was tested on day 4). Adolescent animals were handled at least twice before behavioural testing to get them acclimated to the experimenters. The full experimental timeline is shown in Fig. 1 (Created with BioRender.com).

2.5. Acoustic startle response

Acclimation: Startle testing was performed as described by Valsamis and Schmid (2011). In brief, rats were initially acclimated to the experimental procedure, Plexiglas animal holders, and startle chambers (Med Associates, Vermont, USA) by undergoing three 5 min acclimation sessions, at least 6 h apart. During acclimation, the animals were exposed to a 65 dB sound pressure level (SPL) white noise background sound which is consistently present throughout all startle testing procedures. The animal holders were washed with water and unscented soap between tests for all the startle tests described in this section.

Startle Reactivity: After the acclimation sessions, startle reactivity in response to startle stimuli of varying intensities was measured. This startle reactivity test consisted of 15 white noise startle stimuli, 13 of which were 20 ms in duration, at intensities ranging from 65 to 120 dB SPL in 5 dB increments, presented in a pseudorandomized order. The 110 dB SPL stimulus was presented twice because this was the startle stimulus sound level used for subsequent testing of prepulse inhibition. Two additional white noise stimuli corresponded to the prepulses presented in the PPI test (4 ms duration, 75 or 85 dB SPL). Based on data from the startle reactivity session, platform sensitivity was adjusted for each rat to optimally detect the startle reflex using the full dynamic range without reaching saturation. The adjusted platform gain for each rat was used throughout all the remaining testing sessions.

Habituation: Following startle reactivity testing, animals underwent four consecutive days of startle habituation testing to assess startle reactivity, short-term habituation (STH) and long-term habituation (LTH). Each day, animals were exposed to a 5 min acclimation period with background noise, followed by a habituation block of 30 trials. In the habituation block, each trial consisted of a 20 ms-long, 100 dB SPL white noise stimulus after which the peak-to-peak maximum startle amplitude was measured. Trials were separated by a fixed inter-trial interval (ITI) of 60 s.

PPI: On the fifth day, both habituation and PPI were measured in separate blocks. The habituation block consisted of 20 startle trials using 110 dB SPL stimulus intensity. In the PPI block, animals were exposed to either startle-only trials, with stimulus parameters the same as those in the habituation block, or prepulse trials, in a pseudorandomized order. Prepulse trials included a 4 ms long white noise prepulse of either 75 or 85 dB SPL preceding the startle stimulus by an interstimulus interval (ISI) of either 30 or 100 ms. ISI was determined as the time between the onset of the prepulse to the onset of the startle stimulus. In total, the 40 prepulse trials were divided into ten of each of the following prepulse (dB SPL)/ISI (ms) combinations: 75/30, 75/100, 85/30, and 85/100. The trials were separated by a 12–18 s randomized ITI. Peak-to-peak maximum startle amplitudes were measured. PPI was calculated as the amount of inhibition of startle in prepulse trials compared to startle-only trials in the PPI block:

$$\%PPI\cdot = \cdot\left[1 - \left(\frac{average\ startle\ magnitude\ with\ prepulse}{average\ startle\ without\ prepulse}\right)\right]\cdot \times \cdot 100.$$

Habituation scores were calculated to measure STH. The 30 trials from day 1 of habituation testing were binned into 6 blocks of 5 trials and the STH score was calculated as follows:

$$STH\ score = \frac{Average\ startle\ amplitude\ on\ block\ 6}{Average\ startle\ amplitude\ on\ block\ 1}$$

Based on the calculations above, a score over 1 indicates sensitization and a score below 1 indicates habituation. This value is not biased by changes in baseline startle as it is calculated for each animal and therefore compares their individual baseline to their post-habituation startle amplitude. A score was also calculated to quantify LTH by taking the ratio of block 1 amplitude on day 4 to block 1 amplitude on day 1.

2.6. Social behaviour testing

Each rat's preference for a conspecific over an inanimate object (sociability), as well as its preference for a stranger rat over a familiar rat (social novelty), were assessed using the previously established 3-chamber assay (Crawley, 2007; Moy et al., 2004; Scott et al., 2020). The apparatus was 115 cm long, 58 cm wide, with transparent walls that were 45 cm high. The apparatus was split equally into 3 chambers separated by walls with a gate in the middle (10 cm). The gate was open throughout the test, and test animals were free to explore and move between chambers during the test. In each of the side chambers, a Plexiglass animal holder was placed, which either contained another (stranger of familiar) rat or was left empty. Only one animal was tested at a time. The experimenter was present in the room during the test but was separated from the apparatus by a long divider and could only observe the apparatus through a computer situated 3–4m away connected to the tracking camera. It was not possible to generate age-matched stranger animals to be used for adolescent offspring testing and therefore sex-matched, strain-matched adult strangers were used throughout all social behaviour tests.

The test rat was habituated to the apparatus for 10 min with empty animal holders already positioned in each side chamber. Following habituation, sociability preference was determined by placing a stranger rat (stranger 1) in an animal holder and into one of the side chambers. Then, the test rat's exploration was measured using video monitoring (10 min). Then, social novelty preference was determined in a similar manner by placing a novel stranger rat (stranger 2) in an animal holder and into the opposing side chamber (10 min). During the social novelty stage, stranger 1 is considered the familiar rat, and stranger 2 is considered the novel rat. Between different test rats, the animal holders were washed with unscented soap and the entire apparatus was wiped with 70% ethanol. The test rat's exploration was tracked using a camera and its activity in each chamber was quantified using ANYMAZE software (V4.99, Stoelting, Wood Dale, IL, USA). Additionally, the animal's exploration of the animal holders was tracked, which was specified as the animal's nose being within 3 cm around the animal holder. A sociability or social novelty score was calculated by subtracting the time spent exploring the novel social animal holder ([stranger 1] – [empty animal holder] in sociability; [stranger 2] – [stranger 1] in social novelty). To ensure these scores were not influenced by exposure to ketamine anesthesia 2 days prior, we compared the sociability and social novelty scores of littermates and found no difference in social behaviour scores between animals who were exposed to ketamine anesthesia during ABR testing and their littermates that did not undergo ABR testing.

2.7. Open field test

Rats were placed in a 45.7 cm square open field for 30 min as described previously (Fulcher et al., 2020). This test was used to determine locomotor activity by measuring the total distance traveled throughout the duration of test. Additionally, anxiety-like behaviour was measured through the time spent in the centre of the chamber (15.7 cm square in the centre of the open field). The animal's head location was monitored by an overhead camera as they freely explored the box; the data was collected and analyzed using ANYMAZE software. The apparatus was cleaned with 70% ethanol between experiments.

2.8. Auditory brainstem response

The level of sound-evoked electrical activity in the brainstem was measured using an established protocol (Scott et al., 2018) to assess hearing sensitivity, neural responsivity, and speed of neurotransmission in adolescent and adult rats. Rats were anesthetized with ketamine (80 mg/kg, i.p.) and xylazine (5 mg/kg, i.p.) and placed in a sound-attenuating chamber. Subdermal electrodes (27 gauge; Rochester Electro-Medical, Lutz, FL, USA) were positioned at the vertex (active electrode), over the right mastoid process (reference electrode), and on the midback (ground electrode). Throughout the electrophysiological assessment, body temperature was maintained at 37 °C using a homeothermic heating pad (507220F; Harvard Apparatus, Kent, UK). A click (0.1 ms) stimulus was used in ABR assessment which was generated using a Tucker-Davis Technologies (TDT, Alachua, FL, USA) RZ6 processing module sampled at 100 kHz. A magnetic speaker (MF1; TDT) positioned 5 cm from the animal's right ear was used to deliver the stimuli while its left ear was blocked with a custom foam plug. The acoustic stimuli were each presented 1000 times (21 times/s) at decreasing intensities from 90 to 50 dB SPL in 5 dB SPL steps and from 50 to 20 dB SPL in 3 dB SPL steps. Before the ABR assessment, the acoustic stimuli were calibrated with custom MATLAB software (The Math-Works, Natick, MA, USA) using a 1/4-inch microphone (2530; Larson Davis, Depew, NY, USA) and preamplifier (2221; Larson Davis). The sound-evoked activity associated with the ABR assessment was collected using a low-impedance head stage (RA4L1; TDT), preamplified and digitized (RA16SD Medusa preamp; TDT), and sent to an RZ6 processing module via a fiber-optic cable. The signal was filtered (100–5000 Hz) and averaged using BioSig software (TDT). The peak amplitudes of each of the characteristic positive waves of the ABR were measured in microvolts above the baseline and the latency of each of these peaks was determined from the stimulus onset. For a wave peak to be analyzed, it must have a preceding and following trough less than its maximum. This resulted in the consistent presence of peaks for waves I–IV at 90 dB SPL.

2.9. Immunostaining

Following adult behavioural testing, a subset of animals that underwent behavioural testing were randomly selected and then perfused with saline followed by 4% paraformaldehyde (PFA). Harvested brains were post-fixed for 1h in 4% PFA and then stored in 30% sucrose at 4 °C. Brains were sliced into 40 μm sections using a freezing microtome (Microm HM 560 M) and stored at −20 °C in cryoprotectant (30% sucrose, 30% ethylene glycol, and 5% of 0.01% sodium azide in 0.1 M phosphate buffer). Two slices containing rostral and caudal sections of the pontine reticular nucleus (PnC; Paxinos and Watson, 2009), respectively, were selected per animal for further analysis. These slices correspond closely to brain sections within the bregma coordinates of −9.00 mm to −10.20 mm rostrocaudally. Before immunostaining procedures and between all incubations, slices were thoroughly rinsed with 0.1M phosphate-buffered saline (PBS). All incubations were performed at room temperature with gentle agitation. Slices were first pre-treated with PBS plus 1% H_2O_2 and blocked with PBS+ (PBS containing 0.4 % Triton-X and 0.1% bovine serum albumin) for 1 hr. Then, slices were incubated overnight with primary guinea pig anti-rat-vGlut2 antibody (Millipore Sigma, Cat. No. AB2251-I, Lot#2983096) in PBS+. The following day, slices were incubated with the secondary biotinylated goat anti-guinea pig antibody (Vector, CA, USA) in PBS+ (1:500) for 1 hr. To visualize the immunostaining, ABC-elite (Vector) diluted in PBS (1:1000) was added for 1 hr, followed by a 10-min incubation with 3, 3′-diaminobenzidine tetrahydrochloride (DAB) solution. Slices were rinsed with PBS and mounted on positively charged slides. Slides were placed in a heated chamber at 37 °C for 30 min then washed with distilled water for 5 min and counterstained with 0.5% Thionin solution for 20s. After the Thionin staining step, slides were washed twice for 5 min in distilled water and then gradually dehydrated in increasing concentrations of ethanol (5 min 70%, 3 min 70%, 3 min 95%). Then, slides were slowly dipped 5 times in 95% ethanol with 0.4% glacial acid, dehydrated for 3 min in 100% ethanol and incubated in CitriSolv (3 min, 5 min) before cover slipping with DPX mounting medium.

2.10. Imaging analysis

Stained images were visualized using a Nikon Eclipse Ni–U upright brightfield microscope at 10x and 40x magnification. Images were taken with a DS-F13 high-definition colour camera and imaging software NIS Elements Color Camera (Nikon). Images of 3454 mm width by 1300 mm height were centred to capture the entirety of the PnC area. Using the rat brain atlas (Paxinos and Watson, 2009), we ensured that the following analysis did not include brain regions surrounding the PnC like the reticulotegmental nucleus of the pons, raphe interpositus nucleus, medial longitudinal fasciculus, and the peritrigeminal zone.

Counting of PnC giant neurons: The following steps were applied to each image to ensure a consistent and automated procedure across all slices. The H DAB vectors option of the colour deconvolution tool of the imaging software was used to decompose each original image into three component images. The image representing the Thionin staining was used for this analysis. First, the image was converted to an 8-bit image. Then, image pixels were differentiated into foreground and background to represent the stained and non-stained PnC regions, respectively. The same threshold value was applied to all images. This threshold was chosen based on the images from the slides with the lightest intensity of staining to ensure that no giant neurons would be missed. To identify potential giant neurons, we applied the Analyze Particle function of ImageJ and saved potential cells as regions of interest. To ensure no giant neurons were missed, our Analyze Particle criteria were set to detect cells smaller than a typical giant neuron. Then, we manually inspected the images and any cell with a cross-body diameter of 35 μm or more was identified and counted as a giant neuron.

Quantification of vGlut2 immunostaining: Previously detected giant neurons were sorted by size and five of the largest 10 neurons from each slice were randomly chosen for further analysis. The choice to sort by size was done to reduce the possibility of choosing a non-giant neuron, given that our staining did not use any specific cell markers. In addition, the random selection ensured that our results were not biased to the largest giant neurons but included relatively smaller giant neurons as well. The same cells were imaged at 63x magnification and each image was deconvoluted using the H DAB option. The purple and brown images representing the Thionin and vGlut2 stain, respectively, were converted to 8-bit images, and thresholds were determined. Then, ImageJ's Analyze Particle feature was used to create the ROI outlining the giant neuron cell body and this ROI was expanded 1.3x horizontally and vertically to ensure it covered the neurons' proximal dendritic processes, which are important to consider when quantifying a presynaptic marker like vGlut2. Finally, the enlarged ROI was applied to the vGlut2 staining image, and the percentage of ROI (giant neuron) area covered by vGlut2 staining was measured and used for statistical analysis.

2.11. Statistical data analysis

Data obtained from the behavioural tests described above were analyzed using IBM SPSS Statistics version 26 and graphed using GraphPad Prism for Windows. Behavioural and ABR data were scanned for extreme outliers (>3 interquartile ranges from the median) using the explore function in SPSS. There were no outliers when the offspring results were split based on genotype, MIA, sex, and litter (maxn = 4). Next, offspring results were split based on genotype, MIA and sex, and one animal was removed for being a consistent outlier across multiple tests and having very high startle reactivity (*WT* Poly I:C male).

For social behaviour experiments, some animals experienced

substantial bouts of inactivity (freezing) during either the sociability test, the social novelty test, or both. This inactivity compromised the sociability and social novelty scores obtained from these tests. Therefore, an exclusion threshold of at least 5 m distance traveled in the duration of the 10 minute test sessions was set, and any animals that traveled under 5 m were excluded from the sociability and social novelty score analysis. This freezing effect, likely due to anxiety when the experimenter was switching animals between different stages of the test, occurred only in males and more frequently in adult animals. For reference, non-freezing adolescent males and adult males traveled an average of 26 and 22 m, respectively, during the 10 min testing sessions. Notably, this phenomenon occurred at a similar rate in all the experimental groups.

The animals used for open field and startle testing were virtually identical across the entire experiment, with the exception of one animal that was sacrificed for brain collection following adolescent testing (*Il15*$^{-/-}$ Saline). Table 1 shows the final animal numbers for each experimental group and within each test.

For each behavioural test, a three or four-way repeated-measures analysis of variance (ANOVA) was conducted separately for adolescent and adult data as most of our measures are inherently influenced by age (e.g. startle amplitude increases with age due to changes in body weight, ABR signal changes with age due to changes in skull thickness and size of the head).

All ANOVAs included genotype, sex and MIA as between-subject factors. Additional within-subject factors were included based on the measure of interest: Stimulus intensity for startle reactivity and ABRs, trial number for short-term habituation of startle, day of testing for long-term habituation of startle, prepulse intensity and interstimulus interval for PPI.

3. Results

3.1. Poly I:C MIA reduced startle reactivity in adult WT offspring and *Il15*$^{-/-}$ offspring showed generally higher startle reactivity than WT animals

In both adolescence and adulthood (Fig. 2), *Il15*$^{-/-}$ offspring exhibited increased startle reactivity when compared to *WT* animals. The main adolescent ANOVA revealed a significant stimulus intensity * genotype interaction (F(3.863, 366.981) = 4.928 p = 0.001), where *Il15*$^{-/-}$ offspring showed significantly higher reactivity at 100, 110, 115, and 120 dB (adjusted p values of 0.01, 0.001, 0.039, and 0.01, respectively). In adulthood, a similar stimulus intensity * genotype interaction was found (F(4.541,1034) = 3.6, p = 0.005), although posthoc testing revealed that this was only significant at 115 dB following adjustment for multiple comparisons (p = 0.038).

Poly I:C treatment did not result in any changes in startle reactivity in adolescence. However, in adulthood, *WT* Poly I:C MIA offspring showed reduced startle reactivity (Fig. 2b). This was shown through a significant stimulus intensity* genotype* MIA interaction (F(4.541, 426.850) = 2.620 p = 0.028). Separate ANOVAs were conducted for each genotype showed a significant stimulus intensity * MIA interaction in *WT*, but not in *Il15*$^{-/-}$ offspring (F(11,429) = 3.095 p = 0.017, pairwise comparisons 85 dB: p = 0.031, 110 dB: p = 0.006, 115 dB: p = 0.037).

3.2. ABR and giant neuron phenotypes cannot fully explain poly I:C-related changes in startle reactvitiy

Given the observed increases in startle reactivity, we wanted to investigate whether these are due to a higher auditory sensitivity. To do so, we measured ABRs in adolescent and adult animals. The amplitude of Wave I of the ABR represents activity at the auditory nerve (Scott et al., 2018), which relays information to the startle-mediating PnC giant neurons (Koch, 1999). Although startle reactivity was increased in adolescent *Il15*$^{-/-}$ offspring compared to *WT* offspring, there were no changes in ABR Wave I amplitude in adolescent *Il15*$^{-/-}$ offspring (Fig. 3b). However, in adult animals, ABR Wave I amplitudes were significantly increased in *Il15*$^{-/-}$ offspring compared to *WT* offspring (stimulus intensity * genotype interaction F(1.491,114.308) = 9.069 p = 0.001; 50 dB p = 0.01, 65 dB p = 0.003, 75 p < 0.001, 85 dB p < 0.001, 90 dB p < 0.001), across stimulus intensities from 50 to 90 dB, whereas increased startle reactivity was only observed at 115 dB (Fig. 3b). Notably, there was a significant genotype * MIA * sex interaction (F(1,77) = 4.947 p = 0.029). When followed with separate ANOVAs split by sex (Genotype*MIA interaction, F(1,40) = 6.804 p = 0.013 in females), and posthoc testing, *WT* Poly I:C females showed significantly higher Wave I amplitudes compared to *WT* saline females across all stimulus intensities (p = 0.021, data not shown).

Since altered sensitivity of peripheral auditory structures could not fully explain increased startle reactivity in *IL 15*$^{-/-}$ animals or decreased startle in *WT* Poly I:C offspring, we investigated the number of startle mediating PnC giant neurons and the glutamatergic synaptic input into PnC giant neurons through presynaptic vGlut2 staining. Neither of these parameters were significantly changed in the brains of adult offspring collected shortly after completion of behavioural testing (Fig. 3c; PnC number: genotype main effect F(1,28) = 0.301 p = 0.588; MIA main effect F(1,28) = 0.621 p = 0.437; genotype*MIA interaction F(1,28) = 0.481 p = 0.494; vGlut2 covered area on giant neurons: genotype main effect F(1,28) = 0.372 p = 0.547; MIA main effect F(1,28) = 0.548 p = 0.465; genotype*MIA interaction F(1,28) = 0.289 p = 0.595).

3.3. Startle habituation is not affected by poly I:C MIA or Il15 knockout

Changes in general startle reactivity can be attributed to either a change in sensitivity to the stimulus or a change in reactivity modulation

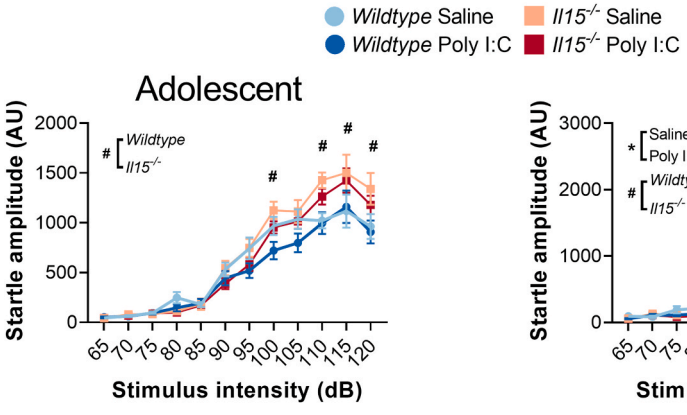

Fig. 2. *WT* but not *Il15*$^{-/-}$ Poly I:C offspring exhibit decreased startle reactivity in adulthood. Regardless of MIA, *Il15*$^{-/-}$ adolescent offspring showed increased startle reactivity at 110, 115, 120 dB compared to *WT* (left graph; # Bonferroni adjusted p values of 0.001, 0.039, and 0.01, respectively). In adulthood, similar to adolescent data, *Il15*$^{-/-}$ offspring had increased reactivity compared to *WT*, but this was only significant for 115 dB stimuli (right graph; # Bonferroni adjusted p value of 0.005). *WT* Poly I:C offspring, but not *Il15*$^{-/-}$ Poly I:C offspring, showed increased startle reactivity at 85, 110, and 115 dB compared to respective saline controls (right graph; * Bonferroni adjusted p values of 0.031, 0.006, and 0.037, respectively). Data are shown as mean ± standard error. For animal numbers per group, please refer to Table 1.

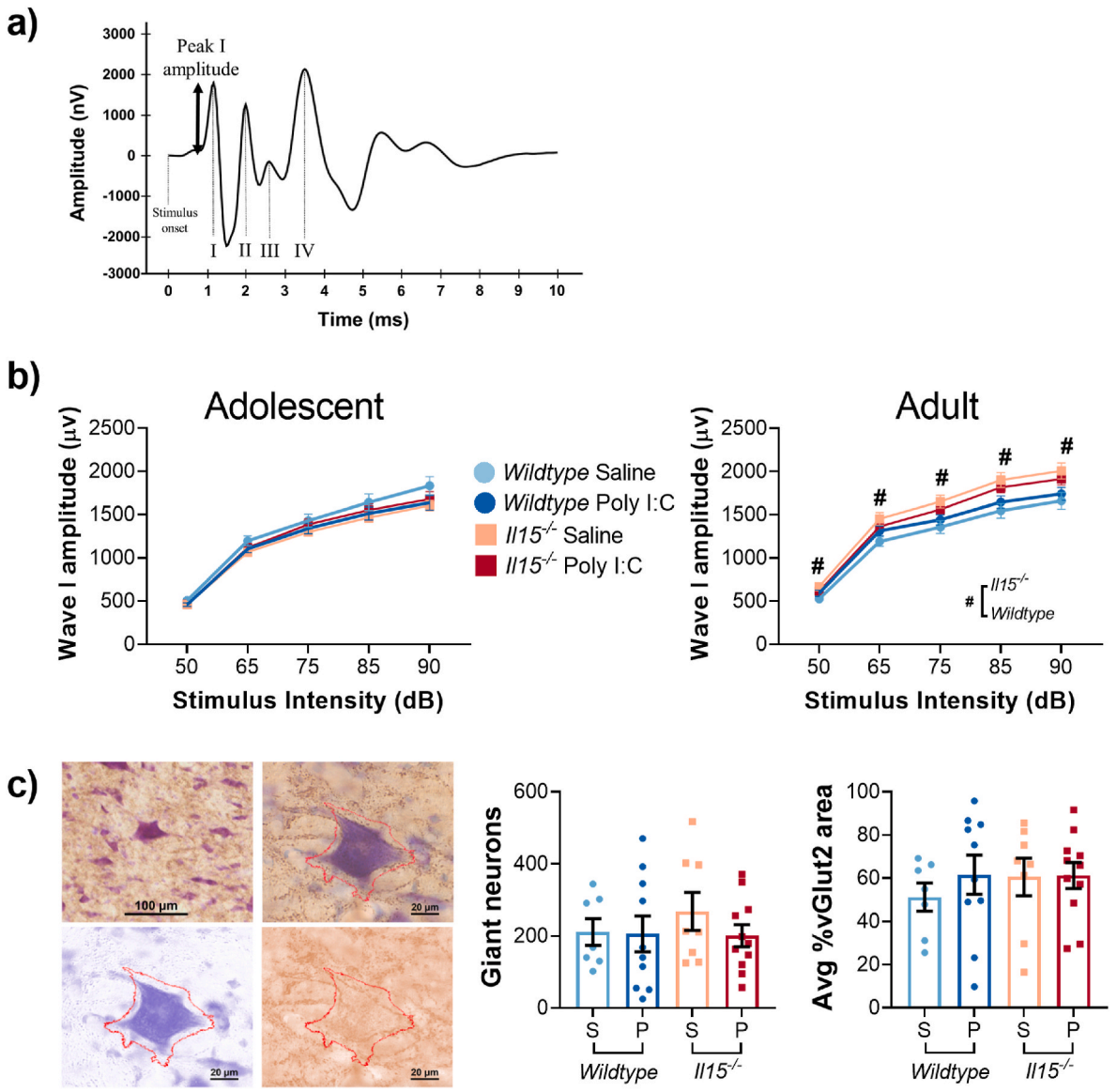

Fig. 3. Wave I amplitudes of auditory brainstem responses, the number PnC giant neurons. and giant neuron presynaptic vGLUT2 immunoreactivity. a) Schematic showing a composite of the raw ABR trace created by averaging the individual measurements taken from all adult *WT* Saline animals in response 90 dB SPL click stimulus. The double headed arrow shows the measurement of ABR Wave I amplitude representing activity at the level of the auditory nerve, which relays information to the startle reflex circuit. *b)* In adolescence (left graph), there was no difference in ABR Wave I amplitude, measured at 5 different stimulus intensities in Poly I:C MIA offspring or in *Il15*$^{-/-}$ animals. In adulthood (right graph), amplitudes across stimulus intensities were higher in *Il15*$^{-/-}$ animals compared to *WT* (# Bonferroni adjusted p values: 50 dB p = 0.01, 65 dB p = 0.003, 75 dB p < 0.001, 85 dB p < 0.001, 90 dB p < 0.001). c) Individual dots represent individual animals. Left panel shows a visualization of the process of identifying giant neurons and the area surrounding each PnC giant neuron where vGlut2 staining was quantified. Neither giant neuron number nor vGlut2 density were affected by Poly I:C MIA or *Il15* knockout. Data are shown as mean ± standard error. For animal numbers per group, please refer to Table 1.

through the processes of habituation and sensitization (Koch, 1999). Our initial reactivity experiment was designed to detect baseline changes in startle reactivity while minimizing the effects of habituation and sensitization by using a small number of stimuli. In the following experiment, we measured the modulation of startle over 6 blocks of 5 trials. We used the ratio of startle amplitude in the last block to the amplitude in the first block to quantify STH (ratio <1) or sensitization (ratio >1).

Our analysis comparing startle reactivity across blocks revealed no significant differences in STH between genotypes or treatment in adolescence (Fig. 4b; adolescent STH score: genotype main effect F(1,95) = 0.710 p = 0.402; MIA main effect F(1,95) = 1.02 p = 0.315; genotype*MIA interaction F(1,95) = 1.07 p = 0.303). A one-sample *t*-test revealed that on average, adolescent animals all showed substantial STH with a score of less than 1 (t(102) = -2.254, p = 0.026). In adulthood, the raw STH score values suggested that adult animals in general did not habituate (one sample *t*-test t(101) = 0.294, p = 0.769)), and a univariate ANOVA confirmed that this was not different between Poly I:C MIA and *Il15*$^{-/-}$ groups (Fig. 4c, adult STH score: genotype main effect F(1,94) = 3.30 p = 0.073; MIA main effect F(1,94) = 0.004 p = 0.947; genotype*MIA interaction F(1,94) = 0.585 p = 0.446)). The lack of STH may have been partly due to our choice of long ITIs (1 min) and the use of block 6 in calculating the STH score (some animals sensitize near the end of the testing session). In addition to STH, we also measured LTH over the 4 habituation days by calculating a score that compares

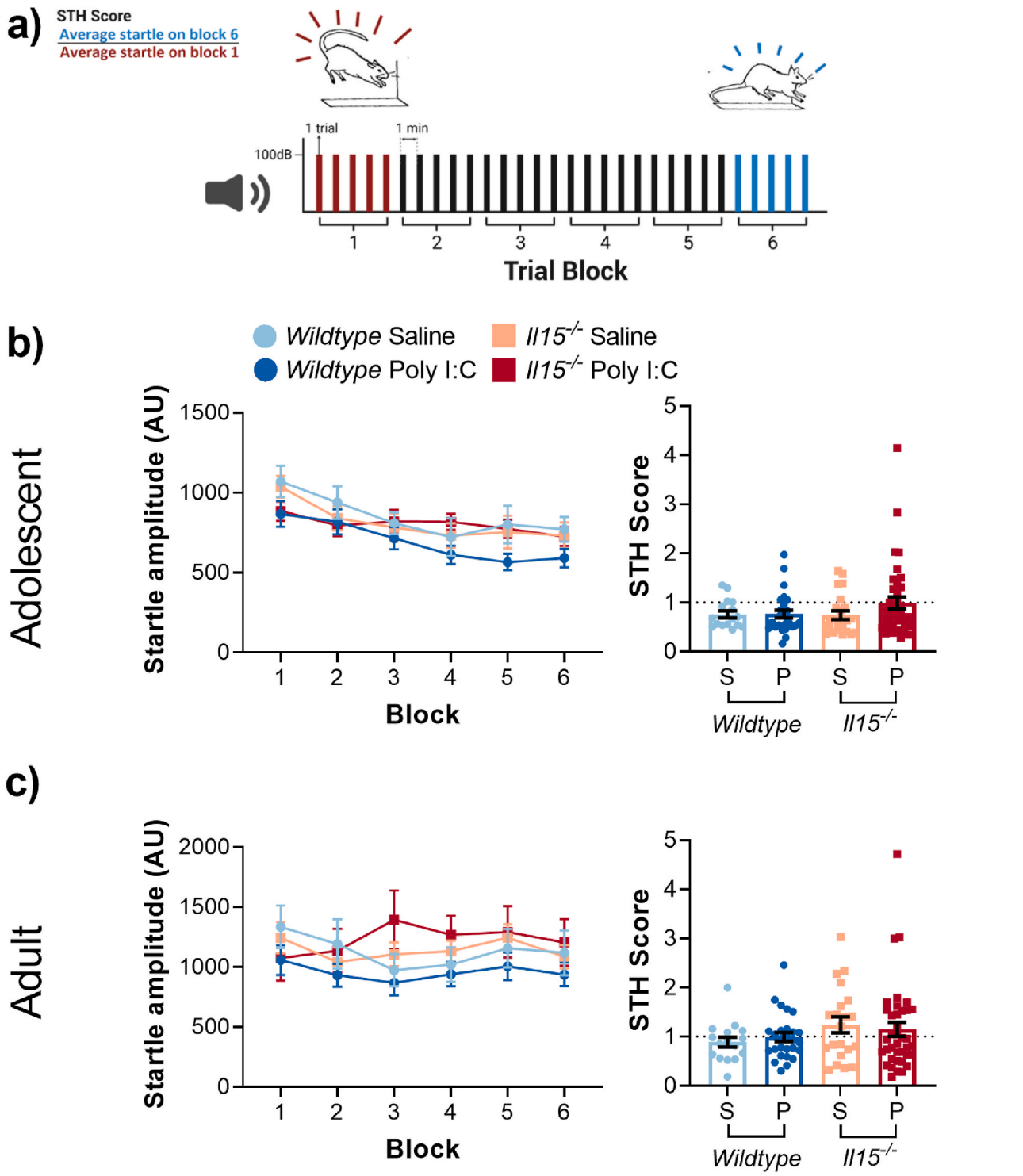

Fig. 4. No differences in short-term habituation following Poly I:C MIA or *Il15* knockout. a) Visual summary of the short-term habituation experiment, highlighting the trials used to calculate STH scores. In b) and c), The two left panels show startle reactivity across 6 blocks of 5 trials each, and the right panels shows the habituation score calculated as a ratio of block 6 to block 1. b) In adolescence, neither genotype nor Poly I:C MIA alters the habituation curves or the habituation score. c) In adulthood, habituation score values suggest that none of the 4 groups habituated well (values overlapping with a score of 1) and there were no significant differences between the groups. Data are shown as mean ± standard error, individual dots represent individual animals. For animal numbers per group, please refer to Table 1.

block 1 startle on day 4 to block 1 startle on day 1. Univariate ANOVAs conducted for each age did not reveal any significant effects related to genotype or MIA for the LTH score (adolescent LTH score: genotype main effect $F(1,95) = 1.446$ $p = 0.232$; MIA main effect $F(1,95) = 0.078$ $p = 0.781$; genotype*MIA interaction $F(1,95) = 0.076$ $p = 0.783$; adult LTH score: genotype main effect $F(1,94) = 0.460$ $p = 0.499$; MIA main effect $F(1,94) = 0.130$ $p = 0.719$; genotype*MIA interaction $F(1,94) = 0.980$ $p = 0.325$).

3.4. Prepulse inhibition of startle

PPI is an operational cross-species measure of sensorimotor gating that is extensively used in both clinical and preclinical studies of psychiatric disorders . Our PPI analysis revealed age-specific effects: PPI was influenced by the *Il15* genotype in adolescence, but was not influenced by genotype in adulthood. A separate repeated-measures ANOVA was conducted for each age point, and the adolescent ANOVA revealed a 3-way prepulse * genotype * MIA interaction ($F(1,95) = 6.014$ $p = 0.016$), which was then followed up by two ANOVAs split by genotype to reveal a prepulse * MIA interaction in *Il15*$^{-/-}$ offspring ($F(1,56) = 9.078$) $p = 0.004$. Posthoc comparison revealed a significant decrease in PPI in adolescent *Il15*$^{-/-}$ animals at 75 dB prepulses ($p = 0.012$; Fig. 5b). In adulthood, the main ANOVA revealed separate findings for each *Il15*$^{-/-}$ and Poly I:C MIA. There was a main effect of Poly I:C ($F(1,94) = 8.381$ $p = 0.005$), whereby Poly I:C offspring showed higher PPI regardless of genotype or prepulse-ISI combination (Fig. 5c). Moreover, there was a significant prepulse * genotype * sex interaction ($F(1,94) = 4.930$ $p = 0.02$), which was followed up with separate ANOVAs split by sex to reveal a significant effect of genotype in males where male *Il15*$^{-/-}$ offspring had higher PPI regardless of prepulse-ISI condition compared to *WT* males (not shown).

3.5. Open field test

In addition to PPI, the open field test is another common test performed in preclinical models of neurodevelopmental disorders. The test has two main readouts: locomotor activity and anxiety-like behaviour. Separate univariate ANOVAs were conducted for each of the two open field measures at each age point.

In adolescence, the main ANOVA for distance traveled revealed significant independent effects of Poly I:C ($F(1,95) = 9.163$, $p = 0.003$) and *Il15* knockout ($F(1,95) = 18.015$, $p < 0.005$) on the total distance traveled. More specifically, adolescent Poly I:C offspring showed decreased distance traveled and *Il15*$^{-/-}$ offspring showed increased distance traveled (Fig. 6a, left panel). In contrast, the main ANOVA for centre time showed a significant main effect of Il15 knockout ($F(1,95) = 4.128$, $p = 0.045$) in addition to a genotype * MIA interaction ($F(1,95) = 9.341$, $p = 0.003$). *Il15*$^{-/-}$ offspring showed a general increase in centre time independent of MIA status ($p = 0.045$), however, the interaction revealed that Poly I:C significantly decreased centre time in *Il15*$^{-/-}$ offspring compared to saline *Il15*$^{-/-}$ offspring (Bonferroni adjusted $p = 0.001$; Fig. 6a, right panel).

In adulthood, the increased distance traveled and centre time in *Il15*$^{-/-}$ offspring independent of MIA status was also present as a main

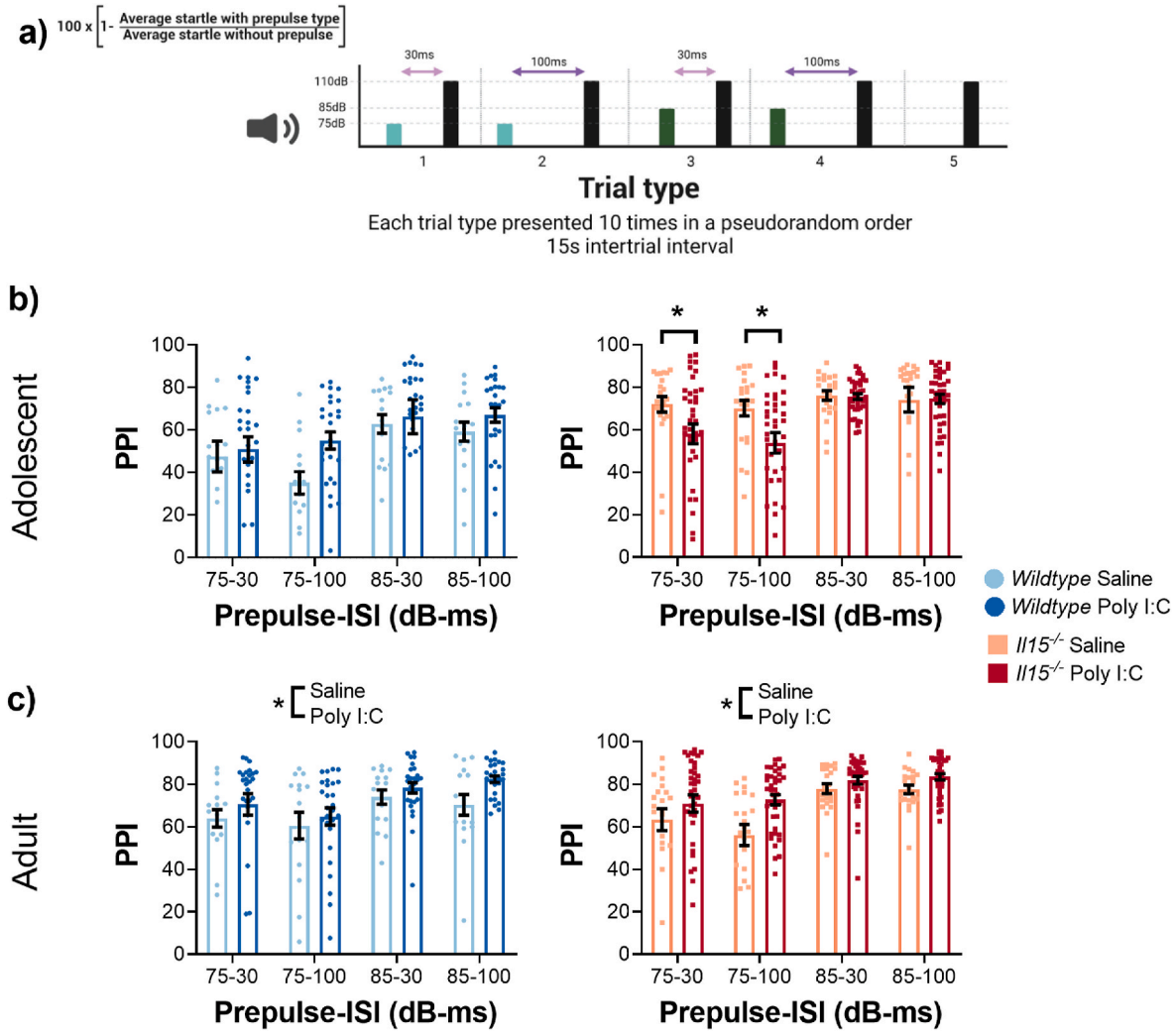

Fig. 5. Poly I:C MIA leads to reduced PPI with a quiet prepulse in adolescent *Il15*$^{-/-}$ offspring and increases PPI regardless of genotype in adulthood. a) Visual summary of the PPI experiment, highlighting the trials and trial types used to calculate PPI. PPI was measured across 4 conditions with 2 prepulses and 2 ISIs. b) In adolescence, *Il15*$^{-/-}$ Poly I:C offspring showed reduced PPI with the 75 dB prepulse regardless of ISI (* Bonferroni adjusted $p = 0.012$). c) In adulthood, there was a main effect of Poly I:C MIA, where Poly I:C offspring had increased PPI regardless of genotype or prepulse-ISI condition (*$p = 0.005$). Data are shown as mean ± standard error, individual dots represent individual animals. For animal numbers per group, please refer to Table 1.

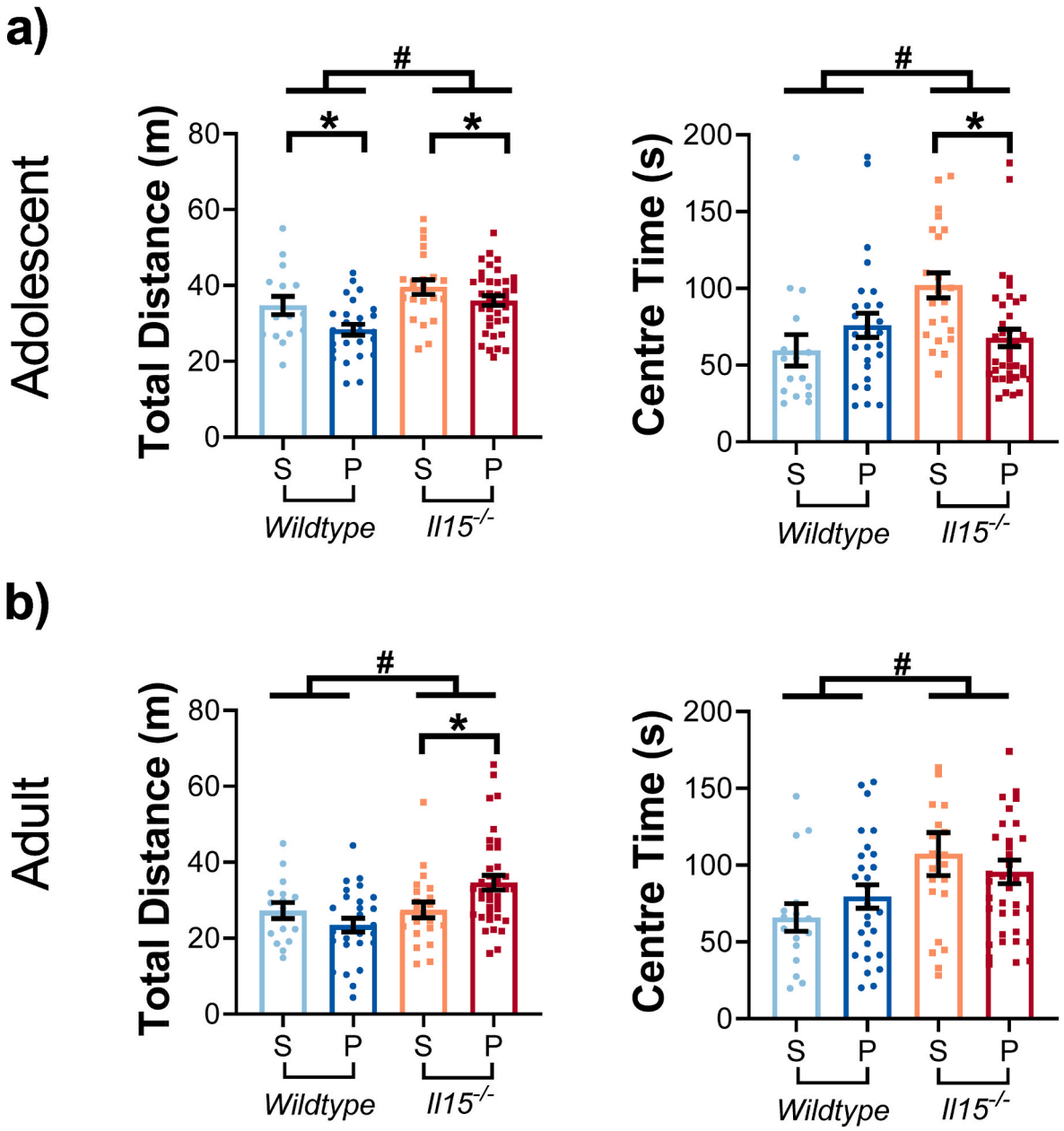

Fig. 6. Effects of Poly I:C and IL15 knockout on locomotor behaviour. a) In adolescence, total distance traveled (left panel) was increased in *Il15*$^{-/-}$ (#p < 0.001) and decreased in Poly I:C offspring (*p = 0.003). The right panel shows that adolescent *Il15*$^{-/-}$ offspring also generally showed increased centre time (#p = 0.045), however, Poly I:C reduced centre time in adolescent *Il15*$^{-/-}$ but not *WT* offspring (* Bonferroni adjusted p = 0.001). b) In adulthood, *Il15* knockout also increased both total distance and centre time (# total distance p = 0.004). Additionally, *Il15*$^{-/-}$ Poly I:C offspring showed significantly increased locomotor activity compared to *Il15*$^{-/-}$ saline offspring (* Bonferroni adjusted p = 0.016). Data are shown as mean ± standard error, individual dots represent individual animals. For animal numbers per group, please refer to Table 1.

effect of genotype (total distance F(1,94) = 8.632, p = 0.004; centre time F(1,94) = 8.512, p = 0.004; Fig. 6b, genotype effects marked by #). In addition, there was a significant genotype * MIA interaction for locomotor activity (F(1,94) = 6.695, p = 0.011), and posthoc testing showed a significant further increase in distance traveled by *Il15*$^{-/-}$ Poly I:C offspring compared to *Il15*$^{-/-}$ saline offspring (* Bonferroni adjusted p = 0.006; Fig. 6b, left panel).

3.6. Social behaviour

Finally, we tested social behaviour using a 3-chamber apparatus. The values used to generate this score were that of specific exploration of the animal holders (test animal head < 3 cm away from the holder) and not exploration of the entire side chamber. A sociability score was determined that reflects the preference of animals to a conspecific over an empty animal holder. In contrast, social novelty reflects the preference for a stranger rat over a familiar rat. All groups showed substantial sociability and social novelty exploration, as shown in Fig. 7 with all scores and their error bars positioned above the zero line. A univariate ANOVA conducted for each test at each age point did not show any main effects or interactions involving genotype and MIA (adolescent sociability score: genotype main effect F(1,87) = 0.906 p = 0.344; MIA main effect F(1,87) = 2.758 p = 0.100; genotype*MIA interaction F(1,87) = 3.430 p = 0.067; adult sociability score: genotype main effect F(1,74) = 2.796 p = 0.099; MIA main effect F(1,74) = 0.210 p = 0.648; genotype*MIA interaction F(1,74) = 1.263 p = 0.265; adolescent social novelty:

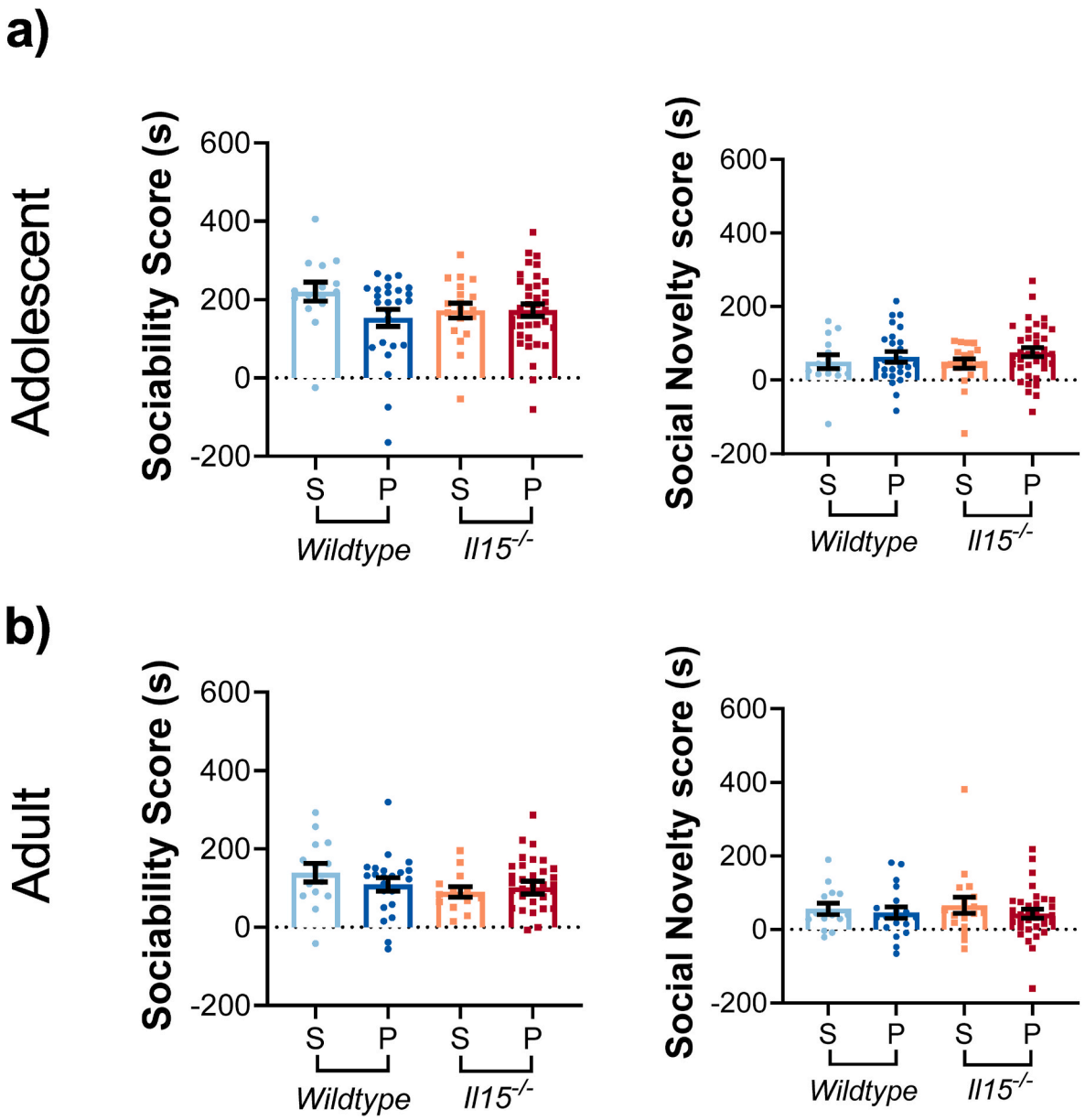

Fig. 7. Neither Poly I:C MIA nor *Il15* deficiency altered social behaviour in adolescence or adulthood. Social behaviour data is shown as sociability and social novelty scores. a) Neither genotype, Poly I:C MIA, nor an interaction between them influenced sociability and social novelty scores in adolescence. b) Adult data shows similar results as in adolescence with no significant differences between any of the groups. Data are shown as mean ± standard error, individual dots represent individual animals. For animal numbers per group, please refer to Table 1.

genotype main effect $F(1,89) = 0.154$ $p = 0.696$; MIA main effect $F(1,89) = 2.194$ $p = 0.142$; genotype*MIA interaction $F(1,89) = 0.140$ $p = 0.709$; adult social novelty: genotype main effect $F(1,76) = 0.157$ $p = 0.693$; MIA main effect $F(1,76) = 1.650$ $p = 0.203$; genotype*MIA interaction $F(1,76) = 0.305$ $p = 0.582$). Therefore, our results show that neither Poly I:C MIA nor *Il15*$^{-/-}$ influence social exploration measured through the 3-chamber test.

3.7. Summary of effects observed in *Il15*$^{-/-}$ rats

While the goal of this study was to explore the interaction of *Il15* knockout with poly I:C MIA, it is also the first study to describe the behavioural phenotype of *Il15*$^{-/-}$ rats. Interestingly, throughout our experiments we observed effects of *Il15* knockout on offspring behaviour or ABR phenotypes independently from Poly I:C MIA. These findings are summarized in Table 2. and support previous evidence pointing towards a role for Il15 in neurodevelopment.

4. Discussion

The findings of this study show that Poly I:C MIA and *Il15* genetic deficiency are two factors that can independently alter offspring behavioural phenotypes. In addition to the effects that each factor had on its own, some of the effects of Poly I:C were dependent on whether animals were *WT* or *Il15*-deficient.

4.1. Genotype effects independent of Poly I:C MIA

Since this novel rat strain was only established recently (Renaud et al., 2017), its behavioural phenotype had not yet been described. *Il15* deficiency led to behavioural and auditory brainstem changes regardless of whether offspring were exposed to Poly I:C MIA. These data are

Table 2
Summary of Il15$^{-/-}$

Phenotype	Genotype effect	Relevant figures or statistics
Increased Startle reactivity	Adolescent *Il15*$^{-/-}$ > *WT* at 95, 110, 115, 120 dB Adult Il15$^{-/-}$ > *WT* at 115 dB	Fig. 2
Increased ABR Wave I amplitude	Adult *Il15*$^{-/-}$ > *WT* at 50, 65, 75, 85, 90 dB	Fig. 3
Increased Locomotor activity	*Il15*$^{-/-}$ > *WT*	Fig. 6
Increased *centre time in the open field*	*Il15*$^{-/-}$ > *WT*	Fig. 6
Shorter ABR Wave IV latency	Adolescent and adult *Il15*$^{-/-}$ < *WT* at 50, 65, 75, 85, 90 dB	Adolescent ($F(1,78) = 13.229$; $p < 0.001$ Adult $F(1,77) = 27.288$; $p < 0.001$
Shorter ABR Wave I-IV interpeak latency	Adolescent and adult *Il15*$^{-/-}$ < *WT* at 50, 65, 75, 85, 90 dB	Adolescent $F(1,78) = 12.971$; $p < 0.001$ Adult $F(1,76) = 33.51$; $p < 0.001$

summarized in Table 2 and they support the involvement of Il15 in brain and behaviour, be it directly through its role in the brain, or indirectly through its proinflammatory roles or the role of NK cells throughout the maternal body, particularly in the uterus.

While our study is the first to report brain and behavioural changes in *Il15*$^{-/-}$ rat offspring, the presence of Il15 in human tissues as well as mouse knockout studies support the role of Il15 as a regulator of neurodevelopment and behavioural responses. For example, *Il15* gene expression has been detected in human fetal astrocytes, microglia, and various neural cell lines (Hanisch et al., 1997; Lee et al., 1996; Satoh et al., 1998). Il15 protein has also been detected throughout the early postnatal and adult mouse brain, with particularly high levels in the hippocampus and cerebellum (Gómez-Nicola et al., 2008). Behavioural results linked to *Il15*-deficiency in earlier studies have been exclusively reported in mice (*Il15* or *Il15R* knockout models), and showed increased conditioned fear, enhanced working memory, increased depressive behaviour, and altered activity during the light phase of the circadian cycle (He et al., 2010a, 2010b; Wu et al., 2010, 2011). Additionally, a previous study by Wu et al. (2010) reported reduced anxiety in the elevated plus-maze in *Il15*$^{-/-}$ mice. This is similar to our findings of increased hyperactivity and increased centre time in the open field, with the latter indicative of reduced anxiety, as animals that are more anxious in the open field tend to move less frequently away from the walls and avoid crossing the centre of the chamber. While comparisons to mouse Il15 studies support the mechanistic role of Il15 in our study's findings, more research is required in rat models to fully confirm our findings, given the immune and nervous system differences that exist between mice and rats (Hok et al., 2016; Holsapple et al., 2003).

4.2. Poly I:C effects independent of Il15 genotype

The Poly I:C effects that were observed in both *WT* and *Il15*$^{-/-}$ offspring were decreased locomotor activity in adolescence and increased PPI in adulthood. Although Poly I:C studies have previously investigated locomotor activity in GD9.5 offspring, most have tested adult offspring only (Borçoi et al., 2015; U. Meyer et al., 2008; Shi et al., 2003; Tang et al., 2013). In younger offspring closer to the age of our adolescent testing, one study did not find any changes in locomotor activity in the open field following Poly I:C MIA (O'Leary et al., 2014). However, experiments were conducted with mice and animals were left in the open field for 10 min only, compared to 30 min as used in our study, which may have been too short to detect subtle differences in activity.

Our finding of increased PPI stands in contrast to various reports of decreased PPI in GD9.5 Poly I:C offspring (Li et al., 2009; Richetto et al., 2017; Shi et al., 2003; Weber-Stadlbauer et al., 2017). One study has previously reported increased PPI in GD9.5 Poly I:C offspring at low prepulse intensities, but this does not match the general effect that we observed regardless of prepulse level or interstimulus interval (Gonzalez-Liencres et al., 2016). The contrasting results may be in part due to the different prepulse parameters used in our experiment (Haddad et al., 2020a) or species differences between rats and mice, including a different developmental trajectory at GD9.5. Many potential immune mechanisms could be responsible for Poly I:C effects, serving as a reminder for the complexity of the Poly I:C immune response and the roles of various immune factors that are not yet fully understood. Poly I:C is capable of eliciting the activation of various immune pathways (Arrode-Brusés and Brusés, 2012), and factors such as Il1β and macrophage inflammatory protein-1α possess functions that may not overlap with Il15 and could be responsible for mediating the changes seen here.

4.3. Poly I:C effects present in WT but not Il15$^{-/-}$ offspring

The main behavioural finding that was seen in *WT* but not *Il15*$^{-/-}$ offspring was decreased startle reactivity in adulthood. This suggests a late manifestation of symptoms similar to what is seen in schizophrenia and commonly reported in Poly I:C MIA studies, including our own (Haddad et al., 2020b). However, while the timing of the effect is similar, its direction is opposite to what we found previously (Haddad et al., 2020a). Part of this discrepancy may be explained by the different strains that we used in the two studies (Holtzman vs Sprague Dawley). Evidence for the importance of strain in Poly I:C studies is supported by mouse studies showing that offspring from different strains given the same Poly I:C treatment exhibited markedly different behavioural phenotypes in open-field exploration, stereotypic behaviour, and depressive-like behaviour (Morais et al., 2018; Schwartzer et al., 2013). More specific to rats, different rat strains exhibited different extent and variability of serum Il6 response 3 hr following Poly I:C MIA (Murray et al., 2019). Furthermore, strain differences have been shown to influence the antibody response to commensal bacterial antigens and the activation state of NK cells in the experimental autoimmune encephalopathy model of multiple sclerosis (Djuretić et al., 2019; Kovačević-Jovanović et al., 2013). Therefore, it is possible that the same Poly I:C immune challenge produced different effects in each strain despite our effort to keep other experimental variables the same as our previous study.

In *WT* offspring, Poly I:C MIA increases circulating levels of Il15 (Arrode-Brusés and Brusés, 2012; Mattei et al., 2001), which can have neurodevelopmental and proinflammatory effects that ultimately alter fetal brain development. From a neurodevelopmental perspective, Gómez-Nicola et al. (2011) previously showed that Il15 can increase the proliferation of adult neural stem cells in culture and their differentiation into astrocytes. If this effect is similar in the prenatal period, then Poly I:C-mediated elevation of Il15 may decrease the number of cells fated to become neurons, thereby influencing many different brain regions. Alternatively, Poly I:C-mediated elevation of Il15 may influence maternal and fetal immune cells, including fetal microglia. Hanisch et al. (1997) showed that Il15 is overexpressed in activated microglia, and that Il15 blockade reduces microglial proinflammatory gene expression. Increased activation of microglia could increase their synaptic pruning abilities and reduce synaptic density throughout the fetal brain, which can alter neuronal excitability. To link changes in neuronal number and synaptic density more specifically to startle phenotypes, we followed up our startle experiment with ABR testing and histological analysis of PnC giant neurons. Wave I of the ABR represents activity at the auditory nerve, which relays information to PnC giant neurons in the brainstem via the cochlear root nucleus. These giant neurons synapse onto motor neurons to manifest the startle response (Koch, 1999; Lingenhohl and Friauf, 1992, 1994). We hypothesized that a decrease in startle reactivity could be due to decreased neuronal activity at the auditory nerve, decreased glutamatergic input and into PnC giant neurons, or decreased numbers of giant neurons. Contrary to our hypothesis, our results

showed that these 3 phenotypes could not account for the decrease in startle reactivity observed in *WT* but not in Il15$^{-/-}$ offspring. Therefore, it is likely that Poly I:C MIA influences startle reactivity through different mechanisms, such as a change in excitatory or inhibitory drive in PnC neurons.

4.4. Poly I:C effects present in *Il15*$^{-/-}$ but not WT offspring

Some Poly I:C effects were present only in *Il15*$^{-/-}$ offspring. These include decreased adolescent PPI at 75 dB SPL prepulses. A previous GD9.5 Poly I:C study that tested PPI in mice at similar timepoints to our experiment matched our *WT* findings by showing normal PPI at PND35 in Poly I:C offspring (Giovanoli et al., 2016). Therefore, it seems that *Il15*$^{-/-}$ offspring may have increased susceptibility to PPI deficits at younger ages. Similarly, *Il15*$^{-/-}$ offspring were more susceptible to increased anxiety-like behaviour in adolescence and locomotor hyperactivity in adulthood. There are previous reports of GD9.5 Poly I:C showing no change in these phenotypes at similar age-points that once again points to increased susceptibility in *Il15*$^{-/-}$ offspring (Meyer, 2005, 2006; O'Leary et al., 2014).

Given the general proinflammatory roles of Il15, increased susceptibility in *Il15*$^{-/-}$ offspring runs against our initial hypothesis which posited this cytokine as a mediator of Poly I:C MIA. However, different immune mechanisms from the ones described previously may be at play. For instance, Il15 is necessary for the development and maturation of NK cells (Ma et al., 2006). The lack of these cells may leave offspring more vulnerable to postnatal immune insults, which have been linked with brain and behavioural changes in preclinical studies (Ibi et al., 2009; Li et al., 2018). Alternatively, many tissue-resident NK populations play non-immune roles in their designated tissue (Shi et al., 2011). One example is the population of uterine NK cells, the lack of which has been shown to alter placental development in the same transgenic rat model used in our study (Renaud et al., 2017). The lack of these tissue-resident NK cells throughout the body could lead to a variety of organ-specific changes that could make offspring more susceptible to behavioural changes triggered by Poly I:C MIA.

4.5. Limitations and future directions

One of the potential limitations of this study is the relatively small number of dams used to generate offspring for behavioural phenotyping. However, previous findings from our group suggest that the small number of dams may not be a severe of a limitation as previously thought due to the small percentage of phenotype variance attributed to between-litter variability (Haddad et al., 2020a). In addition, our past findings were also used as the basis for always using 4 pups per litter per sex when possible as opposed to only 1 or 2. This practice substantially reduces the probability of obtaining an unreliable representation of a litter's average phenotype.

As it stands, the current study cannot answer the question of whether the findings reported are due to the lack of maternal Il15 or fetal Il15. In the future, similar Poly I:C MIA studies could be conducted using different breeding schemes to answer these intricate questions. For example, pairing homozygous knockout dams with heterozygous fathers or vice versa can give rise to situations where either the mother or the pup possess a working copy of *Il15*. Hsiao and Patterson (2012) used this type of breeding and tracked pup genotype to clarify that Il6 elevation in the placenta is mainly due to maternal Il6 as opposed to fetal Il6.

5. Conclusion

In summary, our findings suggest a complex role for Il15 in the context of Poly I:C MIA. Some Poly I:C phenotypes like decreased startle reactivity were only present in *WT* offspring and therefore seem to be mediated by Il15. Other phenotypes like decreased adolescent PPI were only present in *Il15*$^{-/-}$ offspring, which suggests these animals had increased susceptibility to Poly I:C MIA. Finally, changes like increased latency in the ABR were completely independent of *Il15* genotype, pointing to Poly I:C immune pathways that do not involve Il15. Beyond its modulation of the effects of Poly I:C MIA, our study further supports the notion that Il15 is crucially involved in fetal development and that a deficiency in Il15 can lead to various brain and behavioural changes such as neural transmission in the brainstem and propensity to explore novel environments. Future studies should attempt to target the neural mechanisms underlying the phenotypes observed here or more closely study the involvement of Il15 in the immune response induced by Poly I:C MIA.

References

Abdallah, M.W., Larsen, N., Grove, J., Nørgaard-Pedersen, B., Thorsen, P., Mortensen, E. L., Hougaard, D.M., 2013. Amniotic fluid inflammatory cytokines: potential markers of immunologic dysfunction in autism spectrum disorders. World J. Biol. Psychiatr. 14, 528–538. https://doi.org/10.3109/15622975.2011.639803.

Alleva, D.G., Kaser, S.B., Monroy, M.A., Fenton, M.J., Beller, D.I., 1997. IL-15 functions as a potent autocrine regulator of macrophage proinflammatory cytokine production: evidence for differential receptor subunit utilization associated with stimulation or inhibition. J. Immunol. 159, 2941–2951.

Allswede, D.M., Buka, S.L., Yolken, R.H., Torrey, E.F., Cannon, T.D., 2016. Elevated maternal cytokine levels at birth and risk for psychosis in adult offspring. Schizophr. Res. 172, 41–45. https://doi.org/10.1016/j.schres.2016.02.022.

Arrode-Brusés, G., Brusés, J.L., 2012. Maternal immune activation by poly(I:C) induces expression of cytokines IL-1β and IL-13, chemokine MCP-1 and colony stimulating factor VEGF in fetal mouse brain. J. Neuroinflammation 9. https://doi.org/10.1186/1742-2094-9-83.

Atladóttir, H.Ó., Henriksen, T.B., Schendel, D.E., Parner, E.T., 2012. Using maternally reported data to investigate the association between early childhood infection and autism spectrum disorder: the importance of data source. Paediatr. Perinat. Epidemiol. 26, 373–385. https://doi.org/10.1111/j.1365-3016.2012.01296.x.

Atladóttir, H.Ó., Thorsen, P., Østergaard, L., Schendel, D.E., Lemcke, S., Abdallah, M., Parner, E.T., 2010. Maternal infection requiring hospitalization during pregnancy and autism spectrum disorders. J. Autism Dev. Disord. 40, 1423–1430. https://doi.org/10.1007/s10803-010-1006-y.

Blomström, Å., Karlsson, H., Gardner, R., Jörgensen, L., Magnusson, C., Dalman, C., 2016. Associations between maternal infection during pregnancy, childhood infections, and the risk of subsequent psychotic disorder—a Swedish cohort study of nearly 2 million individuals. Schizophr. Bull. 42, 125–133. https://doi.org/10.1093/schbul/sbv112.

Borçoi, A.R., Patti, C.L., Zanin, K.A., Hollais, A.W., Santos-Baldaia, R., Ceccon, L.M.B., Berro, L.F., Wuo-Silva, R., Grapiglia, S.B., Ribeiro, L.T.C., Lopes-Silva, L.B., Frussa-Filho, R., 2015. Effects of prenatal immune activation on amphetamine-induced addictive behaviors: contributions from animal models. Prog. Neuro Psychopharmacol. Biol. Psychiatr. 63, 63–69. https://doi.org/10.1016/j.pnpbp.2015.05.015.

Brown, A.S., Begg, M.D., Gravenstein, S., Schaefer, C.A., Wyatt, R.J., Bresnahan, M., Babulas, V.P., Susser, E.S., 2004a. Serologic evidence of prenatal influenza in the etiology of schizophrenia. Arch. Gen. Psychiatr. 61, 774–780. https://doi.org/10.1001/archpsyc.61.8.774.

Brown, A.S., Hooton, J., Schaefer, C.A., Zhang, H., Petkova, E., Babulas, V., Perrin, M., Gorman, J.M., Susser, E.S., 2004b. Elevated maternal interleukin-8 levels and risk of schizophrenia in adult offspring. Am. J. Psychiatr. 161, 889–895. https://doi.org/10.1176/appi.ajp.161.5.889.

Brown, A.S., Schaefer, C.A., Wyatt, R.J., Goetz, R., Begg, M.D., Gorman, J.M., Susser, E. S., 2000. Maternal exposure to respiratory infections and adult schizophrenia spectrum disorders: a prospective birth cohort study. Schizophr. Bull. 26, 287–295. https://doi.org/10.1093/oxfordjournals.schbul.a033453.

Brown, A.S., Sourander, A., Hinkka-Yli-Salomäki, S., McKeague, I.W., Sundvall, J., Surcel, H.-M., 2014. Elevated maternal C-reactive protein and autism in a national birth cohort. Mol. Psychiatr. 19, 259–264. https://doi.org/10.1038/mp.2012.197.

Careaga, M., Taylor, S.L., Chang, C., Chiang, A., Ku, K.M., Berman, R.F., Van de Water, J. A., Bauman, M.D., 2018. Variability in PolyIC induced immune response: implications for preclinical maternal immune activation models. J. Neuroimmunol. 323, 87–93. https://doi.org/10.1016/j.jneuroim.2018.06.014.

Clark, B.R., Price, E.O., 1981. Sexual maturation and fecundity of wild and domestic Norway rats (Rattus norvegicus). Reproduction 63, 215–220. https://doi.org/10.1530/jrf.0.0630215.

Clarke, M.C., Tanskanen, A., Huttunen, M., Whittaker, J.C., Cannon, M., 2009. Evidence for an interaction between familial liability and prenatal exposure to infection in the causation of schizophrenia. Aust. J. Pharm. 166, 1025–1030. https://doi.org/10.1176/appi.ajp.2009.08010031.

Crawley, J.N., 2007. Mouse behavioral assays relevant to the symptoms of autism. Brain Pathol. 17, 448–459. https://doi.org/10.1111/j.1750-3639.2007.00096.x.

Debost, J.-C.P.G., Larsen, J.T., Munk-Olsen, T., Mortensen, P.B., Meyer, U., Petersen, L., 2017. Joint effects of exposure to prenatal infection and peripubertal psychological trauma in schizophrenia. Schizophr. Bull. 43, 171–179. https://doi.org/10.1093/schbul/sbw083.

Djuretić, J., Pilipović, I., Stojić-Vukanić, Z., Leposavić, G., 2019. Natural killer cells as participants in pathogenesis of rat experimental autoimmune encephalomyelitis

(EAE): lessons from research on rats with distinct age and strain. Cent. Eur. J. Immunol. 44, 337–356. https://doi.org/10.5114/ceji.2019.92777.
Ellman, L.M., Deicken, R.F., Vinogradov, S., Kremen, W.S., Poole, J.H., Kern, D.M., Tsai, W.Y., Schaefer, C.A., Brown, A.S., 2010. Structural brain alterations in schizophrenia following fetal exposure to the inflammatory cytokine interleukin-8. Schizophr. Res. 121, 46–54. https://doi.org/10.1016/j.schres.2010.05.014.
Fang, S.-Y., Wang, S., Huang, N., Yeh, H.-H., Chen, C.-Y., 2015. Prenatal infection and autism spectrum disorders in childhood: a population-based case–control study in taiwan. Paediatr. Perinat. Epidemiol. 29, 307–316. https://doi.org/10.1111/ppe.12194.
Fitzgerald, K.A., McWhirter, S.M., Faia, K.L., Rowe, D.C., Latz, E., Golenbock, D.T., Coyle, A.J., Liao, S.-M., Maniatis, T., 2003. IKKε and TBK1 are essential components of the IRF3 signaling pathway. Nat. Immunol. 4, 491–496. https://doi.org/10.1038/ni921.
Fulcher, N., Azzopardi, E., De Oliveira, C., Hudson, R., Schormans, A.L., Zaman, T., Allman, B.L., Laviolette, S.R., Schmid, S., 2020. Deciphering midbrain mechanisms underlying prepulse inhibition of startle. Progress in Neurobiol. 185, 101734 https://doi.org/10.1016/j.pneurobio.2019.101734.
Giovanoli, S., Weber-Stadlbauer, U., Schedlowski, M., Meyer, U., Engler, H., 2016. Prenatal immune activation causes hippocampal synaptic deficits in the absence of overt microglia anomalies. Brain Behav. Immun. 55, 25–38. https://doi.org/10.1016/j.bbi.2015.09.015.
Goldstein, J.M., Cherkerzian, S., Seidman, L.J., Donatelli, J. -a. L., Remington, A.G., Tsuang, M.T., Hornig, M., Buka, S.L., 2014. Prenatal maternal immune disruption and sex-dependent risk for psychoses. Psychol. Med. 44, 3249–3261. https://doi.org/10.1017/S0033291714000683.
Gómez-Nicola, D., Valle-Argos, B., Pallas-Bazarra, N., Nieto-Sampedro, M., 2011. Interleukin-15 regulates proliferation and self-renewal of adult neural stem cells. Mol. Biol. Cell 22, 1960–1970. https://doi.org/10.1091/mbc.E11-01-0053.
Gómez-Nicola, D., Valle-Argos, B., Pita-Thomas, D.W., Nieto-Sampedro, M., 2008. Interleukin 15 expression in the CNS: blockade of its activity prevents glial activation after an inflammatory injury. Glia 56, 494–505. https://doi.org/10.1002/glia.20628.
Gonzalez-Liencres, C., Juckel, G., Esslinger, M., Wachholz, S., Manitz, M.-P., Brüne, M., Friebe, A., 2016. Emotional contagion is not altered in mice prenatally exposed to poly (I:C) on gestational day 9. Front. Behav. Neurosci. 10 https://doi.org/10.3389/fnbeh.2016.00134.
Haddad, F.L., Lu, L., Baines, K.J., Schmid, S., 2020a. Sensory filtering disruption caused by poly I:C - timing of exposure and other experimental considerations. Brain, Behavior, & Immunity - Health 9, 100156. https://doi.org/10.1016/j.bbih.2020.100156.
Haddad, F.L., Patel, S.V., Schmid, S., 2020b. Maternal immune activation by poly I:C as a preclinical model for neurodevelopmental disorders: a focus on autism and schizophrenia. Neurosci. Biobehav. Rev. 113, 546–567. https://doi.org/10.1016/j.neubiorev.2020.04.012.
Han, V.X., Patel, S., Jones, H.F., Dale, R.C., 2021. Maternal immune activation and neuroinflammation in human neurodevelopmental disorders. Nat. Rev. Neurol. 1–16. https://doi.org/10.1038/s41582-021-00530-8.
Hanisch, U.K., Lyons, S.A., Prinz, M., Nolte, C., Weber, J.R., Kettenmann, H., Kirchhoff, F., 1997. Mouse brain microglia express interleukin-15 and its multimeric receptor complex functionally coupled to Janus kinase activity. J. Biol. Chem. 272, 28853–28860. https://doi.org/10.1074/jbc.272.46.28853.
He, Y., Hsuchou, H., Wu, X., Kastin, A.J., Khan, R.S., Pistell, P.J., Wang, W.-H., Feng, J., Li, Z., Guo, X., Pan, W., 2010a. Interleukin-15 receptor is essential to facilitate GABA transmission and hippocampal-dependent memory. J. Neurosci. 30, 4725–4734. https://doi.org/10.1523/JNEUROSCI.6160-09.2010.
He, Y., Wu, X., Khan, R.S., Kastin, A.J., Cornelissen-Guillaume, G.G., Hsuchou, H., Robert, B., Halberg, F., Pan, W., 2010b. IL-15 receptor deletion results in circadian changes of locomotor and metabolic activity. J. Mol. Neurosci. 41, 315–321. https://doi.org/10.1007/s12031-009-9319-z.
Hok, V., Poucet, B., Duvelle, É., Save, É., Sargolini, F., 2016. Spatial cognition in mice and rats: similarities and differences in brain and behavior. WIREs Cognit. Sci. 7, 406–421. https://doi.org/10.1002/wcs.1411.
Holsapple, M.P., West, L.J., Landreth, K.S., 2003. Species comparison of anatomical and functional immune system development. Birth Defects Res. B Dev. Reprod. Toxicol. 68, 321–334. https://doi.org/10.1002/bdrb.10035.
Hornig, M., Bresnahan, M.A., Che, X., Schultz, A.F., Ukaigwe, J.E., Eddy, M.L., Hirtz, D., Gunnes, N., Lie, K.K., Magnus, P., Mjaaland, S., Reichborn-Kjennerud, T., Schjølberg, S., Øyen, A.-S., Levin, B., Susser, E.S., Stoltenberg, C., Lipkin, W.I., 2018. Prenatal fever and autism risk. Mol. Psychiatr. 23, 759–766. https://doi.org/10.1038/mp.2017.119.
Hsiao, E.Y., Patterson, P.H., 2012. Placental regulation of maternal-fetal interactions and brain development. Development. Neurobiol. 72, 1317–1326. https://doi.org/10.1002/dneu.22045.
Ibi, D., Nagai, T., Kitahara, Y., Mizoguchi, H., Koike, H., Shiraki, A., Takuma, K., Kamei, H., Noda, Y., Nitta, A., Nabeshima, T., Yoneda, Y., Yamada, K., 2009. Neonatal polyI:C treatment in mice results in schizophrenia-like behavioral and neurochemical abnormalities in adulthood. Neurosci. Res. 64, 297–305. https://doi.org/10.1016/j.neures.2009.03.015.
Jiang, H., Xu, L., Shao, L., Xia, R., Yu, Z., Ling, Z., Yang, F., Deng, M., Ruan, B., 2016. Maternal infection during pregnancy and risk of autism spectrum disorders: a systematic review and meta-analysis. Brain Behav. Immun. 58, 165–172. https://doi.org/10.1016/j.bbi.2016.06.005.
Jones, K.L., Croen, L.A., Yoshida, C.K., Heuer, L., Hansen, R., Zerbo, O., DeLorenze, G.N., Kharrazi, M., Yolken, R., Ashwood, P., Water, J.V. de, 2017. Autism with intellectual disability is associated with increased levels of maternal cytokines and chemokines during gestation. Mol. Psychiatr. 22, 273–279. https://doi.org/10.1038/mp.2016.77.
Juraska, J.M., Willing, J., 2017. Pubertal onset as a critical transition for neural development and cognition. Brain Res. 1654, 87–94. https://doi.org/10.1016/j.brainres.2016.04.012. Adolescence as a critical period for developmental plasticity.
Kennedy, M.K., Glaccum, M., Brown, S.N., Butz, E.A., Viney, J.L., Embers, M., Matsuki, N., Charrier, K., Sedger, L., Willis, C.R., Brasel, K., Morrissey, P.J., Stocking, K., Schuh, J.C.L., Joyce, S., Peschon, J.J., 2000. Reversible defects in natural killer and memory Cd8 T cell lineages in interleukin 15–deficient mice. J. Exp. Med. 191, 771–780. https://doi.org/10.1084/jem.191.5.771.
Khandaker, G.M., Zimbron, J., Lewis, G., Jones, P.B., 2013. Prenatal maternal infection, neurodevelopment and adult schizophrenia: a systematic review of population-based studies. Psychol. Med. 43, 239–257. https://doi.org/10.1017/S0033291712000736.
Kim, S., Kim, H., Yim, Y.S., Ha, S., Atarashi, K., Tan, T.G., Longman, R.S., Honda, K., Littman, D.R., Choi, G.B., Huh, J.R., 2017. Maternal gut bacteria promote neurodevelopmental abnormalities in mouse offspring. Nature 549, 528–532. https://doi.org/10.1038/nature23910.
Koch, M., 1999. The neurobiology of startle. Progress in Neurobiol. 59, 107–128. https://doi.org/10.1016/S0301-0082(98)00098-7.
Koks, N., Ghassabian, A., Greaves-Lord, K., Hofman, A., Jaddoe, V.W.V., Verhulst, F.C., Tiemeier, H., 2016. Maternal C-reactive protein concentration in early pregnancy and child autistic traits in the general population. Paediatr. Perinat. Epidemiol. 30, 181–189. https://doi.org/10.1111/ppe.12261.
Korenbrot, C.C., Huhtaniemi, I.T., Weiner, R.I., 1977. Preputial separation as an external sign of pubertal development in the male Rat1. Biol. Reprod. 17, 298–303. https://doi.org/10.1095/biolreprod17.2.298.
Kovačević-Jovanović, V., Miletić, T., Stanojević, S., Mitić, K., Dimitrijević, M., 2013. Strain differences in the humoral immune response to commensal bacterial antigens in rats. Acta Microbiol. Immunol. Hung. 60, 271–288. https://doi.org/10.1556/AMicr.60.2013.3.4.
Lammert, C.R., Frost, E.L., Bolte, A.C., Paysour, M.J., Shaw, M.E., Bellinger, C.E., Weigel, T.K., Zunder, E.R., Lukens, J.R., 2018. Cutting edge: critical roles for microbiota-mediated regulation of the immune system in a prenatal immune activation model of autism. J. Immunol. 201, 845–850. https://doi.org/10.4049/jimmunol.1701755.
Lee, Y.B., Satoh, J., Walker, D.G., Kim, S.U., 1996. Interleukin-15 gene expression in human astrocytes and microglia in culture. Neuroreport 7, 1062–1066.
Li, Q., Cheung, C., Wei, R., Hui, E.S., Feldon, J., Meyer, U., Chung, S., Chua, S.E., Sham, P.C., Wu, E.X., McAlonan, G.M., 2009. Prenatal immune challenge is an environmental risk factor for brain and behavior change relevant to schizophrenia: evidence from MRI in a mouse model. PLoS One 4, e6354. https://doi.org/10.1371/journal.pone.0006354.
Li, Y., Missig, G., Finger, B.C., Landino, S.M., Alexander, A.J., Mokler, E.L., Robbins, J.O., Manasian, Y., Kim, W., Kim, K.-S., McDougle, C.J., Carlezon, W.A., Bolshakov, V.Y., 2018. Maternal and early postnatal immune activation produce dissociable effects on neurotransmission in mPFC–amygdala circuits. J. Neurosci. 38, 3358–3372. https://doi.org/10.1523/JNEUROSCI.3642-17.2018.
Lingenhohl, K., Friauf, E., 1994. Giant neurons in the rat reticular formation: a sensorimotor interface in the elementary acoustic startle circuit? J. Neurosci. 14, 1176–1194. https://doi.org/10.1523/JNEUROSCI.14-03-01176.1994.
Lingenhohl, K., Friauf, E., 1992. Giant neurons in the caudal pontine reticular formation receive short latency acoustic input: an intracellular recording and HRP-study in the rat. J. Comp. Neurol. 325, 473–492. https://doi.org/10.1002/cne.903250403.
Lipina, T.V., Zai, C., Hlousek, D., Roder, J.C., Wong, A.H.C., 2013. Maternal immune activation during gestation interacts with Disc1 point mutation to exacerbate schizophrenia-related behaviors in mice. J. Neurosci. 33, 7654–7666. https://doi.org/10.1523/JNEUROSCI.0091-13.2013.
Lodolce, J.P., Boone, D.L., Chai, S., Swain, R.E., Dassopoulos, T., Trettin, S., Ma, A., 1998. IL-15 receptor maintains lymphoid homeostasis by supporting lymphocyte homing and proliferation. Immunity 9, 669–676. https://doi.org/10.1016/S1074-7613(00)80664-0.
Ma, A., Koka, R., Burkett, P., 2006. Diverse functions of il-2, il-15, and il-7 in lymphoid homeostasis. Annu. Rev. Immunol. 24, 657–679. https://doi.org/10.1146/annurev.immunol.24.021605.090727.
Mandal, A., Viswanathan, C., 2015. Natural killer cells: in health and disease. Hematol. Oncol. Stem Cell Ther. 8, 47–55. https://doi.org/10.1016/j.hemonc.2014.11.006.
Mattei, F., Schiavoni, G., Belardelli, F., Tough, D.F., 2001. IL-15 is expressed by dendritic cells in response to type I IFN, double-stranded RNA, or lipopolysaccharide and promotes dendritic cell activation. J. Immunol. 167, 1179–1187. https://doi.org/10.4049/jimmunol.167.3.1179.
Meyer, U., 2006. The time of prenatal immune challenge determines the specificity of inflammation-mediated brain and behavioral pathology. J. Neurosci. 26, 4752–4762. https://doi.org/10.1523/JNEUROSCI.0099-06.2006.
Meyer, U., Feldon, J., Schedlowski, M., Yee, B.K., 2005. Towards an immuno-precipitated neurodevelopmental animal model of schizophrenia. Neurosci. Biobehav. Rev. 29, 913–947. https://doi.org/10.1016/j.neubiorev.2004.10.012.
Meyer, U., Murray, P.J., Urwyler, A., Yee, B.K., Schedlowski, M., Feldon, J., 2008. Adult behavioral and pharmacological dysfunctions following disruption of the fetal brain balance between pro-inflammatory and IL-10-mediated anti-inflammatory signaling. Mol. Psychiatr. 13, 208–221. https://doi.org/10.1038/sj.mp.4002042.
Meyer, Urs, Nyffeler, M., Yee, B.K., Knuesel, I., Feldon, J., 2008. Adult brain and behavioral pathological markers of prenatal immune challenge during early/middle and late fetal development in mice. Brain Behav. Immun. 22, 469–486. https://doi.org/10.1016/j.bbi.2007.09.012.
Morais, L.H., Felice, D., Golubeva, A.V., Moloney, G., Dinan, T.G., Cryan, J.F., 2018. Strain differences in the susceptibility to the gut–brain axis and neurobehavioural

alterations induced by maternal immune activation in mice. Behav. Pharmacol. 1. https://doi.org/10.1097/FBP.0000000000000374.
Mortensen, P.B., Nørgaard-Pedersen, B., Waltoft, B.L., Sørensen, T.L., Hougaard, D., Torrey, E.F., Yolken, R.H., 2007. Toxoplasma gondii as a risk factor for early-onset schizophrenia: analysis of filter paper blood samples obtained at birth. Biol. Psychiatr. 61, 688–693. https://doi.org/10.1016/j.biopsych.2006.05.024.
Moy, S.S., Nadler, J.J., Perez, A., BArbaro, R.P., Johns, J.M., Magnuson, T.R., Piven, J., Crawley, J.N., 2004. Sociability and Preference for Social Novelty in Five Inbred Strains: an Approach to Assess Autistic-like Behavior in Mice, pp. 287–302. https://doi.org/10.1111/j.1601-183X.2004.00076.x.
Murray, K.N., Edye, M.E., Manca, M., Vernon, A.C., Oladipo, J.M., Fasolino, V., Harte, M. K., Mason, V., Grayson, B., McHugh, P.C., Knuesel, I., Prinssen, E.P., Hager, R., Neill, J.C., 2019. Evolution of a maternal immune activation (mIA) model in rats: early developmental effects. Brain Behav. Immun. 75, 48–59. https://doi.org/10.1016/j.bbi.2018.09.005.
O'Leary, C., Desbonnet, L., Clarke, N., Petit, E., Tighe, O., Lai, D., Harvey, R., Waddington, J.L., O'Tuathaigh, C., 2014. Phenotypic effects of maternal immune activation and early postnatal milieu in mice mutant for the schizophrenia risk gene neuregulin-1. Neuroscience 277, 294–305. https://doi.org/10.1016/j.neuroscience.2014.06.028.
Paraschivescu, C., Barbosa, S., Lorivel, T., Glaichenhaus, N., Davidovic, L., 2020. Cytokine changes associated with the maternal immune activation (MIA) model of autism: a penalized regression approach. PLoS One 15, e0231609. https://doi.org/10.1371/journal.pone.0231609.
Paxinos, G., Watson, C., 2009. The Rat Brain in Stereotaxic Coordinates. Elsevier, Amsterdam; Boston.
Perera, P.-Y., Lichy, J.H., Waldmann, T.A., Perera, L.P., 2012. The role of interleukin-15 in inflammation and immune responses to infection: implications for its therapeutic use. Microb. Infect. 14, 247–261. https://doi.org/10.1016/j.micinf.2011.10.006.
Piekarski, D.J., Johnson, C.M., Boivin, J.R., Thomas, A.W., Lin, W.C., Delevich, K., Galarce, E.M., Wilbrecht, L., 2017. Does puberty mark a transition in sensitive periods for plasticity in the associative neocortex? Brain Res. 1654, 123–144. https://doi.org/10.1016/j.brainres.2016.08.042. Adolescence as a critical period for developmental plasticity.
Pineda, E., Shin, D., You, S.J., Auvin, S., Sankar, R., Mazarati, A., 2013. Maternal immune activation promotes hippocampal kindling epileptogenesis in mice: Pineda et al: MIA and Epilepsy. Ann. Neurol. 74, 11–19. https://doi.org/10.1002/ana.23898.
Pratt, L., Ni, L., Ponzio, N.M., Jonakait, G.M., 2013. Maternal inflammation promotes fetal microglial activation and increased cholinergic expression in the fetal basal forebrain: role of interleukin-6. Pediatr. Res. 74, 393–401. https://doi.org/10.1038/pr.2013.126.
Renaud, S.J., Scott, R.L., Chakraborty, D., Rumi, M.A.K., Soares, M.J., 2017. Natural killer-cell deficiency alters placental development in rats. Biol. Reprod. 96, 145–158. https://doi.org/10.1095/biolreprod.116.142752.
Richetto, J., Massart, R., Weber-Stadlbauer, U., Szyf, M., Riva, M.A., Meyer, U., 2017. Genome-wide DNA methylation changes in a mouse model of infection-mediated neurodevelopmental disorders. Biol. Psychiatr. 81, 265–276. https://doi.org/10.1016/j.biopsych.2016.08.010.
Satoh, J., Kurohara, K., Yukitake, M., Kuroda, Y., 1998. Interleukin-15, a T-cell growth factor, is expressed in human neural cell lines and tissues. J. Neurol. Sci. 155, 170–177. https://doi.org/10.1016/S0022-510X(97)00310-9.
Schwartzer, J.J., Careaga, M., Onore, C.E., Rushakoff, J.A., Berman, R.F., Ashwood, P., 2013. Maternal immune activation and strain specific interactions in the development of autism-like behaviors in mice. Transl. Psychiatry 3. https://doi.org/10.1038/tp.2013.16 e240–e240.
Scott, K.E., Kazazian, K., Mann, R.S., Möhrle, D., Schormans, A.L., Schmid, S., Allman, B. L., 2020. Loss of Cntnap2 in the rat causes autism-related alterations in social interactions, stereotypic behavior, and sensory processing. Autism Res. 13, 1698–1717. https://doi.org/10.1002/aur.2364.
Scott, K.E., Schormans, A.L., Pacoli, K.Y., Oliveira, C.D., Allman, B.L., Schmid, S., 2018. Altered auditory processing, filtering, and reactivity in the Cntnap2 knock-out rat model for neurodevelopmental disorders. J. Neurosci. 38, 8588–8604. https://doi.org/10.1523/JNEUROSCI.0759-18.2018.
Shi, F.-D., Ljunggren, H.-G., La Cava, A., Van Kaer, L., 2011. Organ-specific features of natural killer cells. Nat. Rev. Immunol. 11, 658–671. https://doi.org/10.1038/nri3065.
Shi, L., Fatemi, S.H., Sidwell, R.W., Patterson, P.H., 2003. Maternal influenza infection causes marked behavioral and pharmacological changes in the offspring. J. Neurosci. 23, 297–302.
Shin Yim, Y., Park, A., Berrios, J., Lafourcade, M., Pascual, L.M., Soares, N., Yeon Kim, J., Kim, S., Kim, H., Waisman, A., Littman, D.R., Wickersham, I.R., Harnett, M.T., Huh, J.R., Choi, G.B., 2017. Reversing behavioural abnormalities in mice exposed to maternal inflammation. Nature 549, 482–487. https://doi.org/10.1038/nature23909.
Smith, S.E.P., Li, J., Garbett, K., Mirnics, K., Patterson, P.H., 2007. Maternal immune activation alters fetal brain development through interleukin-6. J. Neurosci. 27, 10695–10702. https://doi.org/10.1523/JNEUROSCI.2178-07.2007.
Solek, C.M., Farooqi, N., Verly, M., Lim, T.K., Ruthazer, E.S., 2018. Maternal immune activation in neurodevelopmental disorders. Dev. Dynam. 247, 588–619. https://doi.org/10.1002/dvdy.24612.
Sørensen, H.J., Mortensen, E.L., Reinisch, J.M., Mednick, S.A., 2009. Association between prenatal exposure to bacterial infection and risk of schizophrenia. Schizophr. Bull. 35, 631–637. https://doi.org/10.1093/schbul/sbn121.
Tang, B., Jia, H., Kast, R.J., Thomas, E.A., 2013. Epigenetic changes at gene promoters in response to immune activation in utero. Brain Behav. Immun. 30, 168–175. https://doi.org/10.1016/j.bbi.2013.01.086.
Valsamis, B., Schmid, S., 2011. Habituation and prepulse inhibition of acoustic startle in rodents. JoVE, e3446. https://doi.org/10.3791/3446.
Weber-Stadlbauer, U., Richetto, J., Labouesse, M.A., Bohacek, J., Mansuy, I.M., Meyer, U., 2017. Transgenerational transmission and modification of pathological traits induced by prenatal immune activation. Mol. Psychiatr. 22, 102–112. https://doi.org/10.1038/mp.2016.41.
Wu, X., He, Y., Hsuchou, H., Kastin, A.J., Rood, J.C., Pan, W., 2010. Essential role of interleukin-15 receptor in normal anxiety behavior. Brain Behav. Immun. 24, 1340–1346. https://doi.org/10.1016/j.bbi.2010.06.012.
Wu, X., Hsuchou, H., Kastin, A.J., He, Y., Khan, R.S., Stone, K.P., Cash, M.S., Pan, W., 2011. Interleukin-15 affects serotonin system and exerts antidepressive effects through IL15Rα receptor. Psychoneuroendocrinology 36, 266–278. https://doi.org/10.1016/j.psyneuen.2010.07.017.
Zerbo, O., Yoshida, C., Grether, J.K., Van de Water, J., Ashwood, P., Delorenze, G.N., Hansen, R.L., Kharrazi, M., Croen, L.A., 2014. Neonatal cytokines and chemokines and risk of autism spectrum disorder: the early markers for autism (EMA) study: a case-control study. J. Neuroinflammation 11, 113. https://doi.org/10.1186/1742-2094-11-113.